ROCK2/ras^{Ha} cooperation induce malignant conversion via p53 loss, elevated NF-κβ and tenascin C-associated rigidity but p21 inhibits ROCK2/NF-κβ-mediated progression

Siti F Masre[1,3] *Nicola Rath*[2], *Michael F. Olson*[2] *and David A Greenhalgh.*[1,4]

[1]Section of Dermatology and Molecular Carcinogenesis, School of Medicine, Dentistry and Nursing, College of Medical, Veterinary and Life Sciences, Glasgow University G31 2ER;
[2]

Molecular Cell Biology Laboratory, Cancer Research UK, Beatson Institute for Cancer Research, Garscube Estate, Glasgow G61 1BD, UK.
[3]

Biomedical Science Programme, School of Diagnostic and Applied Health Sciences, Faculty of Allied Health Sciences, University of Kebangsaan, Malaysia, 50300 Kuala Lumpur.

[4]Corresponding Author

David A. Greenhalgh, PhD
Section of Dermatology and Molecular Carcinogenesis
Level 2, New Lister Building, University of Glasgow
Glasgow Royal Infirmary
10 Alexandra Parade, Glasgow G31 2ER
[0] 141 201 8621
david.greenhalgh@glasgow.ac.uk

RUNNING TITLE: ras/ROCK2 co-operation in transgenic mouse skin

KEY WORDS: transgenic, skin, carcinogenesis, progression, promotion, rigidity

ABSTRACT

To study ROCK2 activation in carcinogenesis, mice expressing 4-hydroxytamoxifen (4HT)-activated *ROCK2* [*K14.ROCK^{er}*] were crossed to mice expressing epidermal activated *ras^{Ha}* [*HK1.ras^{1205}*]. At 8 weeks, 4HT-treated *K14.ROCK^{er}-HK1.ras^{1205}* cohorts exhibited papillomas similar to *HK1.ras*^{1205} controls; however, *K14.ROCK^{er}-HK1.ras^{1205}* histotypes comprised a mixed papilloma/well-differentiated squamous cell carcinoma [wdSCC], exhibiting p53 loss, increased proliferation, and novel NF-κβ expression. By 12 weeks, *K14.ROCK^{er}-HK1.ras^{1205}* wdSCCs exhibited increased NF-κβ and novel tenascin C, indicative of elevated rigidity; yet despite continued ROCK2 activities /p-Mypt1 inactivation, progression to SCC required loss of compensatory p21 expression. *K14.ROCK^{er}-HK1.ras^{1205}* papillomatogenesis also required a wound-promotion stimulus, confirmed by breeding *K14.ROCK^{er}* into promotion-insensitive *HK1.ras^{1276}* mice, suggesting a permissive *K14.ROCK^{er}-HK1.ras^{1205}* papilloma context [wound-promoted/NF-κβ^{+ve}/p53^{-ve}/p21^{+ve}] preceded *K14.ROCK^{er}*-mediated [p-Mypt1/tenascin C/rigidity] malignant conversion. Malignancy depended on ROCK^{er}/p-Mypt1 expression, as cessation of 4HT-treatment induced disorganised tissue architecture and p21-associated differentiation in wdSCCs; yet tenascin C retention in connective tissue ECM suggests the rigidity laid down for conversion persists. Novel papilloma outgrowths appeared expressing intense, basal-layer p21 which confined endogenous ROCK2/p-Mypt1/NF-κβ to supra-basal layers, and was paralleled by restored basal-layer p53. In later SCCs, 4HT-cessation became irrelevant as endogenous ROCK2 expression increased, driving progression via p21 loss, elevated NF-κβ expression and tenascin C-associated rigidity; with p-Mypt1 inactivation/actinomyosin-mediated contractility to facilitate invasion. However, p21-associated inhibition of early-stage malignant progression and the intense expression in papilloma outgrowths, identifies a novel, significant antagonism between *p21* and *ras^{Ha}/ROCK2/NF-κβ* signalling in skin

carcinogenesis. Collectively these data show that ROCK2 activation induces malignancy in ras^{Ha}-initiated/promoted papillomas in the context of p53 loss and novel NF-κβ expression; whilst increased tissue rigidity and cell motility/contractility help mediate tumour progression.

INTRODUCTION

ROCK2, an effector of RhoA signalling downstream of ras^{Ha}, plays essential roles in the regulation of actomyosin contraction and cellular tension during normal regulation of proliferation and differentiation.[1,2] ROCK2 acts to regulate cellular motility through phosphorylation of LIM kinases (LIMK), myosin regulatory light chains (MLC2) and myosin-binding subunit to inhibit MLC phosphatase (Mypt1). Thus in carcinogenesis, deregulated ROCK2 signalling and Mypt1 inactivation increases actomyosin-mediated cellular tension and collagen deposition that alters the extracellular matrix [ECM] to increase tissue rigidity,[3-8] alongside increased cell contractibility/motility that facilitates invasion.[4-6] This increased matrix density changes integrin clustering and increases proliferation via signalling through FAK downregulates GSK3β and increases β-catenin;[5,6] whilst additional signal transduction pathways[9-12] provide a matrix permissive for tumour progression.[4-6,13]

This association with invasion and metastasis, plus the fact that ROCK proteins act as effectors downstream of ras signalling, make ROCK inhibition an attractive therapeutic target;[3,8] particularly since ras-specific inhibitors have proved unsuccessful.[14] However, few transgenic studies have directly explored activated ROCK2/ras^{Ha} synergism. Classic DMBA/TPA skin carcinogenesis employing 4HT-inducible *ROCK2* mice [*K14.ROCK^{er}*][15] implicated synergism with ras^{Ha} activation[16] as papilloma conversion rates increased;[5] but given the numerous mutations elicited by DMBA initiation[16] direct *ROCK2*/*ras^{Ha}* co-operation remains unclear and potential synergism in earlier papillomatogenesis uncertain. Thus, to ratify *ras/ROCK2* synergism, identify stage-specific causality and explore the unfolding progression mechanism, 4HT-inducible *K14.ROCK^{er}* mice were bred into a well-characterised model of *ras^{Ha}*-driven mouse skin carcinogenesis.[17-20] Here exclusive epidermal v-ras^{Ha} expression, induces wound-dependent, regression-prone papillomas

[*HK1.ras*^{1205}] or epidermal hyperplasia alone [*HK1.ras*^{1276}];[17] phenotypes ideal to assess ROCK2/ras synergism in papilloma formation and malignant conversion/progression[17-20] and assess effects on epidermal differentiation.[21,22]

In this model, activated ROCK2/ras^{Ha} co-operation induced malignant conversion via p53 loss, increasing the numbers of proliferating cells prone to DNA damage; novel ROCK2-associated increase in NF-κβ expression; and elevated tenascin C, indicative of tissue rigidity. However, earlier ras/ROCK synergism in papilloma aetiology required both ras^{Ha} activation and a [wound] promotion stimulus. Furthermore, compensatory p21 expression in well-differentiated SCCs inhibited early-stage malignancy, requiring p21 loss to progress to aggressive SCC. Cessation of 4HT treatment demonstrated that malignant conversion depended upon continued 4HT-mediated ROCK^{er}/endogenous ROCK2 activation; however novel papilloma outgrowths appeared expressing intense p21 levels in proliferative basal layer keratinocytes that confined [endogenous] ROCK2/p-Mypt1/NF-κβ expression to supra-basal, differentiating layers; accompanied by return of p53 expression to prevent relapse. These data confirm ras^{Ha}/ROCK2 synergism drives both malignant conversion and malignant progression, and identify a significant antagonism between p21 responses following p53 loss and ROCK2/NF-κβ/tenascin C signalling in ras^{Ha} skin carcinogenesis.

RESULTS

ROCK2 activation co-operates with ras^{Ha} to elicit malignant conversion but a tumour promotion stimulus is required to develop papillomas.

To investigate deregulated ROCK2 signalling synergism with ras^{Ha} activation in classic mouse skin carcinogenesis, *K14.ROCK^{er}* mice were initially bred into line *HK1.ras*^{1205} which expressed activated *v-ras^{Ha}* exclusively in transit amplifying keratinocytes of the epidermal basal layer and required a promotion stimulus [TPA/ear-tag wounding] to develop wound-sensitive papillomas that do not spontaneously convert to malignancy.[17-19] In addition to investigate the requirement for wound promotion, *K14.ROCK^{er}* mice were also bred into a wound-insensitive *HK1.ras*^{1276} line which exhibits hyperplasia alone unless treated with TPA or acquires an additional appropriate oncogenic insult.[17-20] In repeat experiments, performed over a 12 month period, cohorts of age-matched, bi-genic *K14.ROCK^{er}/HK1.ras^{1205}*, *HK1.ras^{1205}* and *K14.ROCK^{er}* siblings were treated with 4HT for 8-10wks (n = 12); 10-12wks (n =12) and 14-16wks (n = 8) respectively; with controls [n = 6 per cohort per experiment] receiving ethanol alone [Figure 1a-d]. At 8wks, *K14.ROCK^{er}/HK1.ras^{1205}* and *HK1.ras^{1205}* mice developed papillomas at the wounded ear tag site, with little overt difference between cohorts [Figure 1b vs 3c]. By week 12, in repeat experiments, all 4HT-treated *K14.ROCK^{er}/HK1.ras^{1205}* mice typically exhibited a single keratotic tumour [wdSCC] at the treated and tagged ear site, culminating in larger, less keratotic, reddish tumour [SCC] by 14 weeks; whereas all untreated *K14.ROCK^{er}/HK1.ras^{1205}* or *HK1.ras^{1205}* controls exhibited standard papilloma clusters associated with HK1.ras^{1205} mice [Figure 1a][17-19]. All 4HT-treated *K14.ROCK^{er}/HK1.ras^{1205}* followed this aetiology, unless mice lost the wound promotion stimulus from ear tags and if so regardless of treatment/genotype [n = 9], such tumours remained small or regressed [Figure 1d; Supplementary Figure S1].[17,18] This requirement for a wound-promotion stimulus was directly assessed in 4HT-treated

K14.ROCK^{er}/HK1.ras^{1276} mice [n= 9 per cohort]. In repeat experiments] these mice failed to develop overt papillomas regardless of ear-tag wounding, over the thrice-weekly/20wk treatment regime [Figure 1e]; although hyperplasia did increase in all 4HT-treated *K14.ROCK^{er}/HK1.ras^{1276}* mice [n =18; Supplementary Figure S1].

At 8 weeks, untreated *K14.ROCK^{er}/HK1.ras^{1205}* tumours exhibited a squamous cell papilloma histotype [Figure 1f] indistinguishable from 4HT-treated *HK1.ras* controls, with a well-ordered, sequential keratinocyte differentiation pattern, and strong supra-basal keratin K1 expression [see Figure 3g] indicative of benign tumours.[17-20] However, all 4HT-treated *K14.ROCK^{er}/HK1.ras^{1205}* tumours exhibited a mixed histotype of papilloma and well-differentiated SCC [Figure 1g; n = 24], which by 12 weeks progressed to uniform wdSCCs [Figure 1h; n=24] possessing a disordered basal layer and strands of aggressive SCC [Figure 1i and j]. In repeat experiments, by 14-16wks, all 4HT-treated *K14.ROCK^{er}/HK1.ras^{1205}* tumours [n =16] progressed to aggressive SCC [see figure 2: panel 3]; whereas no evidence of malignant conversion was observed in untreated controls [n = 12] or *HK1.ras* [n =12].[17-19] Malignant conversion to wdSCC was confirmed by reduced keratin K1 expression[17-20] already apparent in 8wk tumours [Figure 1k], which reduced further and was subsequently lost as wdSCCs [Figure 1l] on progressed to K1-negative SCCs [see time course, Figure 2 panel 3]; whilst all control tumours exhibited a suprabasal K1 expression profile consistent with a papilloma histotype.[17-19]

ROCK^{er}/ROCK 2 isoform activation and Mypt1 inactivation drive malignant conversion; but ras^{Ha} activation is required for papillomatogenesis.

To confirm temporal, stage-specific ROCK^{er} expression all biopsies were analysed for GFP^{tag} expression together with endogenous ROCK2; whilst 4HT-mediated ROCK^{er}/ROCK2 activation were confirmed by phosphorylation of Mypt1[1-3] [Figure 2]. Initially pre-malignant

stages were analysed comparing epidermal histotype and GFP^{tag}, p-Mypt and ROCK2 isotype expression in 4HT-treated (Figure 2: Panel 1 a-d) and untreated (e-h) *K14.ROCK^{er}* mice or 4HT-treated *HK1.ras* mice (i-l). As reported previously[5,15] 4HT-treated *K14.ROCK^{er}* mice exhibit mild hyperplasia without signs of papillomatogenesis [20wks], even after prolonged, thrice weekly treatments over nine months [Figure 2: Panel 1a]; whilst *HK1.ras* mice exhibited a more severe epidermal hyperplasia [Figure 2: Panel 1i].[17] Exogenous ROCK^{er} expression was distinguished from endogenous ROCK2 via GFP^{tag} expression, absent in *HK1.ras* controls [Figure 2: Panel 1b and f vs j]. ROCK^{er} activation by 4HT treatment was confirmed via p-Mypt1 expression [Figure 2c] which appeared in all epidermal compartments including basal-layers; consistent with ROCK^{er} expression from the K14 promoter.[15] In untreated controls, p-Mypt1 expression was low/undetectable whilst 4HT-treated, hyperplastic *HK1.ras* epidermis exhibited a low, supra basal p-Mypt1 expression profile [Figure 2: Panel 1k]. Analysis of endogenous ROCK2 expression and in 4HT-treated *K14.ROCK^{er}* cohorts, ROCK2-specific antibodies detected endogenous ROCK2 expression in *spinous* keratinocytes and weaker ROCK^{er} expression in proliferative basal-layers; as shown at a junction between 4HT-treated and untreated skin [Figure 2: Panel 1 d vs h]. Here, 4HT-treated *HK1.ras* epidermis exhibited low, supra-basal ROCK2 expression, consistent with p-Mypt1 staining [Figure 2: Panel 1l]. Given that ROCK2-specific antibodies detected exogenous ROCK^{er} expression in *K14.ROCK^{er}* basal layer keratinocytes following 4HT-treatment whilst untreated skin or hyperplastic *HK1.ras* keratinocytes exhibited endogenous ROCK2 in supra-basal layers, it suggests that 4HT-treatment increased/stabilized ROCK^{er} expression[15] and that ROCK2 functions primarily in differentiated keratinocytes to provided the tensile strength to the *spinous* layers.[21,22] *K14.ROCK^{er}*, *ROCK2* and *HK1.ras* expression profiles in proliferative, keratin mK14^{+ve} basal layers or differentiated, supra-basal, keratin mK1^{+ve} layers are summarised in Figure 2 [diagram 1].

In carcinogenesis, temporal analysis of both GFP^{tag} [Figure 2: Panel 2a and c) and p-Mypt1(2b and f) gave similar results and confirmed K14.ROCK^{er} expression and activation in 4HT-treated *K14.ROCK^{er}/HK1.ras^{1205}* papillomas and carcinomas at 8 and 12 weeks respectively; whilst *HK1.ras^{1205}* papillomas were negative for GFP^{tag} expression and at 12 weeks only low/supra-basal p-Mypt1 expression was observed [Figure 2e and f]. Temporal analysis of ROCK^{er}/ROCK2 isoforms [Figure 2, panel 3a-f] show strong, elevated expression in all epidermal compartments of papillomas [8wks], wdSCCs [12wks] and SCCs [16wks]; whereas 4HT-treated *HK1.ras^{1205}* [12wks] papillomas exhibit weak, supra-basal ROCK2 expression, similar to the levels shown in hyperplasia [panel 1]; consistent with supra-basal p-Mypt1 inactivation [panel 2]. Temporal analysis of keratin mK1 expression [green vs mK14 (red)], employed to aid in histology assessment,[17-20] shows that strong, supra-basal expression in benign *HK1.ras* papillomas becomes reduced in wdSCC/SCC nests and is lost on progression to invasive SCC [Figure 2: panel 3g-i].

p53 loss and increased proliferation predispose to malignant conversion; but persistent p21 correlates with ROCK^{er}-activation to limit early-stage malignant progression

To investigate mechanism(s) underlying *K14.ROCK^{er}/HK1.ras^{1205}* carcinogenesis, a temporal, stage-specific analysis of p53 and p21 status was performed, and proliferation levels were determined via BrdU-labelling [Figure 3: panels 1-3]. At 8wks, treated *K14.ROCK^{er}/HK1.ras^{1205}* tumours exhibited elevated p53 expression, with nuclear expression in basal layer keratinocytes [Figure 3: panel 1a and b], as observed previously in HK1.ras papillomas[20,23] and untreated controls. However, all treated *K14.ROCK^{er}/HK1.ras^{1205}* also exhibited areas of reduced p53 expression not seen in controls, beginning in basal layers giving a weaker, cytoplasmic expression in the post mitotic supra-basal layers [Figure 3: panel 1c]. This expression profile was consistent with their reduced K1 expression and

propensity for malignant conversion [above, Figure 1g and k]; such that by 12wks, 100% of both wdSCCs [n=24]/SCCs [n=24] tested became p53 negative [Figure 3: panel 1d and e].

In contrast, whilst elevated p21 expression was observed in all 4HT-treated and untreated *K14.ROCK^{er}/HK1.ras^{1205}* papillomas [Figure 3: panel 2a][20,23] unlike p53 expression analysis, all 4HT-treated *K14.ROCK^{er}/HK1.ras^{1205}* papillomas and wdSCCs examined to date retained an elevated p21 expression profile [Figure 3: panel 2b-d], with clear persistent p21 expression in wdSCC basal layer nuclei [Figure 3: panel 2d]. This phenotype persisted until over the ensuing 4 week period, such [p21^{+ve}/K1^{+ve}] wdSCCs progressed to [p21^{-ve}/K1^{-ve}] aggressive SCCs as p21 expression was lost; beginning in basal layer cells, again giving a supra-basal, cytoplasmic expression profile in 14wk SCCs [Figure 3: panel 2e]. As p21 expression in wdSCCs often paralleled that of ROCK^{er}-targeted basal layers [Figure 3: panel 2c]; it suggests a direct antagonism between ROCK^{er} signalling and p21, an idea supported by the relative lack of a significant proliferation increase following conversion as determined by BrdU-labelling [below; panel 3]; plus the intriguing, intense p21 expression observed following cessation of 4HT treatment [Figure 5].

Given previous studies detected deregulated ROCK2 signalling effected cell proliferation[5] plus indications of a ROCK^{er}/p21 antagonism, cell proliferation rates were assessed in stage-specific tumours via BrdU labelling [Figure 3: panel 3]. Consistent wild the mild hyperplasia observed, 4HT-treated *K14.ROCK^{er}* epidermis possessed a mitotic index approximately double that in normal 4HT-treated skins [Figure 3: panel 3a,b] but less than HK1.ras epidermis,[17-19] which exhibited a greater degree of hyperplasia [Figure 3: panel 3c], and a labelling similar to untreated/treated HK1.ras papillomas [Figure 3: panel 3d; 22.00±1.75 vs 16.00±1.70] or untreated *K14.ROCK^{er}/HK1.ras^{1205}* controls [19.50±1.70]. In contrast by 8 weeks, 4HT-treated *K14.ROCK^{er}/HK1.ras^{1205}* papillomas possessed a significantly increased

proliferation rate [61.50 ± 1.25; $p<0.05$], consistent with p53 reduction/loss and larger papillomas [Figure 1a vs. d]. This subtle observation identifies a novel, earlier ROCK2/ras^{1205} synergism where increased proliferation results in papillomas prone to malignant conversion; however 4HT-treated *K14.ROCK^{er}/HK1.ras^{1205}* wdSCCs exhibited only a moderate, insignificant increase in mitotic index (71.56±5.25), suggesting that persistent/nuclear p21 expression inhibited proliferation of basal wdSCC keratinocytes to help limit early-stage progression.[20,23,24]

Malignant conversion and early progression depend on continued ROCK^{er}/ROCK2 expression and further highlights antagonism with p21.

An advantage of the 4HT-inducible system is the ability to assess oncogene dependence via cessation of treatment [Figure 4]. Thus, in two cohorts [n=5] at 12 and 14 weeks treatments ceased and tumours were biopsied two weeks later [Figure 4: panel 1]. Typically at 12wks, 4HT-treated *K14.ROCK^{er}/HK1.ras^{1205}* mice exhibited pale, keratotic wdSCCs which by 14wks became larger, less keratotic and well-vascularised, indicative of malignant progression [Figure 4: panel 1a and b]. After two weeks without 4HT, neither cohort exhibited the envisage regression in size, although the 12wk cohort exhibited increased keratosis; and both 12wk and 14wk *K14.ROCK^{er}/HK1.ras^{1205}* cohorts exhibited new tumour outgrowths, necessitating termination [Figure 4: panel 1d and e]; whilst control papilloma clusters changed little during this period [Figure 4: panel 1c and f].

A detailed analysis two weeks post 4HT cessation, found that earlier wdSCC cohorts [12wks] [Figure 4: panel 2a] exhibited areas of disturbed basal-layer architecture, with disorganised keratinocytes and intercellular spaces suggesting a loss of cell-cell integrity [panel 2b] and an increased acanthosis [expansion of the *spinous* layer] suggesting elevated differentiation;

whereas other areas appeared to be progressing to SSC [panel 2a: black vs yellow box]. Increasing K1 expression at these disorganised sites [panel 2c; white vs yellow box] also indicates a differentiation response, consistent with the appearance of elevated, basal layer p21expression[20,23,24] throughout this tumour [panel 2d; black vs yellow box; and 2e]. However, unlike that observed in analysis of papilloma outgrowths [below], in this context p53 expression did not return [panel 2f]; a feature possibly due to elevated NF-κβ expression [see Figure 6] hence the differentiation response rather than aopoptosis.[23] Typically following 4HT cessation, ROCK2 antibody analysis found decreased exogenous $ROCK^{er}$/endogenous ROCK2 expression at these $p21/K1^{+ve}$ sites and here expression became supra-basal also [panel 2g and h]. Nonetheless, such wdSCCs possessed unaffected areas [Figure 4: panel 2a,c and d, yellow boxed areas] which had little K1/p21 and here endogenous, basal-layer ROCK2 expression was detected [panel 2i] and activity confirmed by elevated p-Mypt1 expression [see Figure 7]; suggesting ROCK activation was required to maintain malignancy at this specific wdSCC stage.

Analysis of older *K14.ROCK^{er}/HK1.ras^{1205}* tumours support this conclusion, and as the 14wk tumours example shown [taken at 16wks] comprised highly invasive SCC and residual wdSCC [Figure 4: panel 3a; white vs yellow boxed area) it allowed a direct comparison of SCC and wdSCC within the same tissue section. This demonstrated that K1-negative SCC histotypes had mow lost p21 on progression [Figure 4: panel 3b, c and f] and now exhibited elevated, basal-layer [endogenous] ROCK2 activation as determined by p-Mypt1 expression in the invasive SCC cells [panel 3d,e and g]. In contrast, residual wdSCC areas exhibiting disturbed tissue architecture, again expressed an increased K1/p21 profile and resultant basal-to-supra-basal transition of endogenous ROCK2 expression [panel 3h-j] paralleled by reduced p-Mypt1 inactivation [Figure 7; below]. Thus, during the additional two weeks

before treatment cessation, wdSCCs had progressed to a state where endogenous ROCK2 arose to substitute for 4HT-activated exogenous ROCK^{er} and continued to drive malignant progression, as observed in other tumour types.

The intriguing lack of tumour regression exhibited by *K14.ROCK^{er}/HK1.ras^{1205}* carcinomas following 4HT cessation was unexpected, and the novel tumour outgrowths in particular were carefully re-examined [Figure 5]. Biopsies of all such outgrowths revealed a papilloma histotype, surprisingly devoid of wdSCC/SCC and keratin K1 expression confirmed their benign histotype [Figure 5a-c]. One feature of this analysis was that such tumour outgrowths repeatedly exhibited unusually intense p21 staining [Figure 5d-h], and at these sites of intense p21 expression, another novel feature was the return of p53 re-expression [Figure 5i-l] as observed previously.[23] Indeed, employing standard p21 staining techniques, this intense p21 expression profile appeared unique to these specific *K14.ROCK^{er}/HK1.ras^{1205}* papilloma outgrowths when compared to analysis of similar histotypes [Figure 3 above]. Given that in previous studies western analysis was compromised by varying levels of contaminating connective tissue and keratosis,[23] an attempt to semi-quantify this aspect exploited p21 antibody titration. In several experiments utilising sections from separate outgrowths [n = 6], found that a four-fold anti-p21 dilution (1/200) gave acceptable staining [Figure 5e-g] in all layers, including basal layer nuclei [Figure 5h]. However, whilst similar analysis performed in parallel confirmed the return of p53 expression, again observed in all layer and in basal layer nuclei [Figure 5i-l], the 1/200 anti-p53 dilution repeatedly failed to detect significant expression levels.

Moreover, another striking characteristic was that whilst endogenous ROCK2 levels remained elevated compared to untreated *K14.ROCK^{er}/HK1.ras^{1205}* papillomas [Figure 2: panel 1l and 3d], ROCK2 expression was now strictly confined to differentiated layers in p21

positive papillomas; a result paralleled by supra-basal p-Mypt1 expression [Figure 5m-p]. Collectively these data suggest that malignant conversion depended upon ROCK2 activation; given that 12wk wdSCCs exhibited a dependence on ROCK^{er} to maintain malignancy [Figure 4: panel 2] and 14wk tumours progressed to SCC due to endogenous ROCK2 expression; whilst intense, compensatory p21 staining reinforces the idea of a significant p21-mediated antagonism to *ROCK2*/*ras*^{Ha} synergism in proliferative basal layers, which in this context, enables return of p53 to prevent a relapse into malignancy.[20,23,24]

Analysis of *NF-κβ* expression in *K14.ROCK*^{er}*/HK1.ras*^{1205} carcinogenesis identifies an early, ROCK2-dependent role.

NF-κβ-dependent transcription is a major target of Rho signalling and may contribute to the stromal remodelling that drives tumour progression.[9,10,25] Analysis of *NF-κβ* found that by 8wks, 4HT-treated *K14.ROCK*^{er}*/HK1.ras*^{1205} papillomas exhibited expression in all layers, [Figure 6: panel 1a and b]. By 12wks, expression intensified, becoming prominent in the invasive fronts of wdSCCs, with many nuclear-positive basal-layer keratinocytes [Figure 6: panel 1c and d]. On progression to aggressive SCC, NF-κβ expression became condensed and increasingly nuclear [Figure 6: panel 1e-g], concomitant with increasing endogenous ROCK2 and p21 loss [above]. In contrast, untreated *K14.ROCK*^{er}*/HK1.ras*^{1205} papillomas [12wks; Figure 6: panel 1h] exhibited weak staining, suggesting NF-κβ expression depended upon 4HT-activated ROCK^{er} signalling; an idea also supported by detectable NF-κβ in 4HT-treated *K14.ROCK*^{er} but not *HK1.ras*^{1205} hyperplasia [Figure 6: panel 1i and j] that express low endogenous ROCK2 levels [Figure 2: panel 1g and 3d].

This association of NF-κβ with ROCK2 signalling was reinforced in 4HT-cessation experiments [Figure 6: panel 2]; although some stage-specific differences were observed. For instance, in wdSCC sections the areas of disturbed tissue architecture and increasingly

$p21^{+ve}/K1^{+ve}$ [Figure 4: panel 2a,c and d [black/white boxed areas], retained NF-κβ expression [Figure 6: panel 2a and b] despite the reduction in exogenous $ROCK^{er}$ activation, thus possibly preventing the return of compensatory p53 expression.[25,26] However, the unaffected areas that now expressed elevated, endogenous ROCK 2 [Figure 4: panel 2a,c and d (yellow boxed areas); and 2i] also expressed elevated NF-κβ. Indeed following cessation, analysis of the later SSC [14wk] cohorts, found elevated NF-κβ expression [Figure 6: panel 2c and d] directly paralleled this increased endogenous ROCK2 and was concomitant with reduced p21 [Figure 4: panel 3a-g]. In contrast, intensely $p21^{+ve}$ papilloma outgrowths [Figure 5d-h] exhibited reduced NF-κβ levels with little basal-layer expression [Figure 6: panel 2e and f vs. panel 1b)]; consistent with the restricted, now supra-basal ROCK2 expression [Figure 6: panel 2g]; and thus this reduced NF-κβ may facilitate the return of p53 expression to these papilloma basal layers [Figure 5i-l]. Collectively, these data suggest a $ROCK^{er}$-mediated NF-κβ expression associates with early-stage *K14.ROCK^{er}/HK1.ras^{1205}* papillomatogenesis and may help create the context for malignant conversion via effects on p53 expression[25,26] and appears necessary for continued malignancy, given the observed susceptibility to elevated levels of p21 following cessation of 4HT treatment.

Tenascin C analysis indicates increasing tissue/ECM rigidity associates with malignant conversion, calling for ROCK2-mediated p-Mypt1 expression to facilitate invasion.

In normal tissues, ECM expression of tenascin C is low but levels increase during tumour progression and given the interrelationship between ROCK2-associated collagen deposition and resultant integrin-mediated in the extracellular matrix,[4-6] tenascin C levels were analysed to assess stage-specific roles and whether expression reflected increased tissue stiffness.[27-29] 4HT-treated *K14.ROCK^{er}/HK1.ras^{1205}* papillomas [8wks] expressed low tenascin C levels [Figure 7: panel 1a and b] whereas wdSCC/SCCs exhibited intense staining in carcinoma

tissue and elevated ECM staining in surrounding connective tissue [Figure 7: panel 1c-e]. Contol *HK1.ras*^{1205} papillomas expressed only weak tenascin C levels in connective tissue ECM, but of note, low-level tenascin C expression was routinely detected in dermal ECM of 4HT-treated *K14.ROCK*^{er} hyperplasia unlike that of HK1.ras^{1205} [Figure 7: panel 1f-h]. Following 4HT cessation the 14wk cohorts of aggressive SCC histotypes displayed intense tenascin C expression in both tumour tissue and connective tissue ECM. In contrast, wdSCC histotypes no longer exhibited tenascin C in tumour tissue ECM but of note, repeatedly retained expression in connective tissue/ECM [Figure 7: panel 1i-k]. Novel papilloma outgrowths also possessed only sporadic patches of [supra-basal] tenascin C with weak dermal/ECM staining [Figure 7: panel 1l]. These data show tenascin C expression depended upon ROCK 2 activation and expression appeared significant post p53 loss/conversion; whereas expression in wdSCCs connective tissue ECM post 4HT cessation, suggests that once laid down at conversion, tissue rigidity persists in wdSCCs.

Thus, to assess the requirement for cell contraction/motility on malignant progression p-Mypt1 levels were analysed. As anticipated, in 4HT-treated *K14.ROCK*^{er}*/HK1.ras*^{1205} papillomas, elevated p-Mypt1 expression paralleled ROCK^{er} activation with levels prominent in the invasive fronts/nests of wdSCC/SCCs [above; Figure 7: panel 2a-c]. Following 4HT-cessation, SSC areas show persistent p-Mypt1 expression paralleled increasing endogenous ROCK2 activities [above]; whilst wdSCC histotypes exhibit reduced expression, consistent with a lack of activated exogenous ROCK^{er} [Figure 7: panel 2d and e] and their inability to invade. In addition, whilst papilloma outgrowths displayed elevated p-Mypt1, expression was again confined to super-basal layers, alongside supra-basal ROCK2 due to intense basal-layer p21 expression. Hence, these data suggest that Mypt1 inactivation is necessary to facilitate changes in actinomyosin/MLC essential to give cells the motility necessary for subsequent invasion of tissues with increased rigidity.

DISCUSSION

These data demonstrate direct co-operation between 4HT-inducible ROCK^{er} and *ras*^{Ha} activation, such that by 10 weeks, 100% of *K14.ROCK*^{er}*/HK1.ras*^{1205} papillomas progressed to wdSCC; whereas all untreated cohorts or controls lacked spontaneous malignant conversion.[17-20] This synergism is consistent with accelerating DMBA/TPA chemical carcinogenesis employing *K14.ROCK*^{er} mice[5] and identification of ROCK2-associated p-Mypt1activities in human skin carcinomas[6] and other cancer types.[7,8] 4HT-cessation experiments demonstrated that malignant conversion relied upon continued ROCK^{er} activities, unless endogenous ROCK2 activities arose to maintain progression. Thus, deregulated Rho/ROCK2 activation maybe a common synergistic event in *ras*^{Ha}-initiated carcinogenesis, hence the major efforts geared to developing ROCK inhibitors[3,8] that may achieve the elusive Achilles heel of successful anti-*ras*^{Ha} therapies.[14]

In terms of stage-specific roles, ROCK^{er} acts at the malignant conversion stage in *K14.ROCK*^{er}*/HK1.ras*^{1205} cohorts with one caveat: the appropriate papilloma context had to be achieved prior to malignant conversion. This included reduction/loss of p53; novel NF-κβ expression, together with elevated tenascin C, indicative of altered ECM and increasing tissue stiffness. Another salient feature of *K14.ROCK*^{er}*/HK1.ras*^{1205} papillomatogenesis was the necessity for a promotion stimulus, typically supplied by the ear-tag wounding; and a pre-requisite for papilloma aetiology in *HK1.ras*^{1205} mice.[17-20] Hence, if wound-associated promotion was lost, *K14.ROCK*^{er}*/HK1.ras*^{1205} papillomas regressed. Indeed, the necessity for an appropriate promotion stimulus was demonstrated in *HK1.ras*^{1276} mice, a line insensitive to ear-tag wounding but sensitive to TPA[17,19] and fos activation.[18] Here, 4HT-treated *K14.ROCK*^{er}*/HK1*.ras^{1276} cohorts failed to exhibit papillomas; despite a thrice weekly/20wk treatment regime. Nonetheless, in these 4HT-treated *K14.ROCK*^{er}*/HK1.ras*^{1276} cohorts, the ROCK^{er}-associated alterations in collagen deposition plus integrin/FAK/β-catenin expression

effects,[5,6] resulted in an increased hyperplasia and highlighted an early synergism. However, in this tissue context *K14.ROCK^{er}/HK1.ras^{1276}* synergism did not provide a permissive environment leading to overt papillomas. Hence, new experiments add a constitutive promotion role via *fos* activation[20,30,31] to investigate potential mechanisms of *ROCK2/fos* co-operation.

These data also show that ROCK2 deregulation alone was insufficient to produce tumours requiring *ras^{Ha}*-mediated initiation[5,17] and once in sync, in a permissive papilloma environment, the *K14.ROCK^{er}*-associated features induced malignant conversion. This synergism included a spatial context to tumour progression, as ROCK^{er}/ROCK2-activation in proliferative basal-layer keratinocytes was a prerequisite for malignant conversion and progression; otherwise untreated *K14.ROCK^{er}/HK1.ras^{1205}* and control *HK1.ras^{1205}* papillomas typically displayed a weak endogenous ROCK2 expression profile, with weak p-Mypt1 inactivation confined to post-mitotic, supra-basal layers. Cessation experiments support this idea also, as wdSCCs [12wks] relied on ROCK^{er} activation in proliferative basal cells to maintain malignancy, whereas novel papilloma outgrowths lacked basal-layer ROCK2/p-Mypt1 expression; whilst later SSCs had acquired endogenous ROCK2 activation/p-Mypt1 inactivation in basal layers. Furthermore, as ROCK2 may contribute to intra-cellular tension/rigidity in normal epidermal differentiation giving tensile strength to *spinous*-layer keratinocytes,[21,22] [manuscript in prep], the abrupt loss of basal ROCK^{er} expression following 4HT-cessation may account for the increased differentiation marker expression observed in wdSCCs and alongside p21 expression[23,24] induce a differentiation response; given the lack of p53 to induce apoptosis.[32]

Previously, such compensatory p53/p21 responses were found to be key features in the mechanism underlying malignant conversion and progression in this skin model.[20,23] In respect to p53, all 4HT-treated *K14.ROCK^{er}/HK1.*ras^{1205} cohorts lost expression prior to

conversion, beginning in papilloma basal layers. The increased mitotic index following p53 loss and the lack of DNA repair would give rise to additional mutations in highly proliferative cells giving a susceptibility to malignant conversion.[32,33] Indeed, as outlined below, these *K14.ROCK^{er}/HK1*.ras^{1205} data suggest a mechanism involving p53 loss which links ROCK2-associated NF-κβ deregulation to the matrix remodelling that drives progression[34-37] when coupled to GSK3β/β-catenin/WNT signalling effects.[5,23,38] Overall however, the identification of p21-associated responses may be of most significance, as this appears to limit [early-stage] malignant progression in *K14.ROCK^{er}/HK1.ras^{1205}* carcinogenesis as observed in another version of this model.[20,23] Despite many observations that p21 expression is lost alongside that of p53,[40] as p53 diminished in *K14.ROCK^{er}/HK1.ras^{1205}* papillomas, basal layer p21 expression increased and moreover, persisted in wdSCCs becoming eventually lost on progression to SCC.[20,23,41] All wdSCCs exhibited persistent basal-layer p21 expression, which exactly paralleled K14.ROCK^{er}/p-Mypt1 expression suggesting that increased p21 is a common response to ras/ROCK^{er}/ROCK2 activities. This feature also accounts for malignancy appearing within 10 weeks but progression to SCC required an additional 4-6wks; necessitating both p21 loss and continued ROCK^{er}/ROCK2 activities. A *p21-ras^{Ha}/ROCK2* antagonism is also suggested by the intense p21 expression observed in papilloma outgrowths following cessation of 4HT. Initially, p21 was elevated in *K14.ROCK^{er}/HK1.ras^{1205}* and control papillomas, but appeared mainly supra-basal, consistent with roles in keratinocyte differentiation.[23,24] However, the intense p21 expression was unprecedented[20,23] and appears directly geared to restrict residual ROCK2/p-Mypt1 expression [and NF-κβ; below] to their differentiation roles in post-mitotic, supra-basal keratinocytes.[21,22]

Previous studies support antagonism between *p21* and *ras^{Ha}/ROCK2*-mediated malignant progression[11,42] as *in vitro*, Rho kinases functioned to block ras^{Ha} -induced p21 expression;[11]

yet activated Rho GTPases did not transform NIH3T3 cells; showing the necessity for ras^{Ha} activation.[11] Later studies demonstrated ROCK2 affected cyclin D1 activity by regulating p21 levels[12,42] and given that p21-mediated inhibition of cyclin D1 was observed in tri-genic $ras^{1276}/fos/\Delta 5PTEN^{flx}$ carcinogenesis,[20] this reinforces stage–specific p21 responses to oncogenic signalling, geared to attempted restoration of cell-cycle control; hence the lack of a significant increase in mitotic index in $K14.ROCK^{er}/HK1.ras^{1205}$ wdSCCs compared to papillomas. Subsequently, as p21 dissipates during malignant progression, attempts to maintain chromosomal stability following p53 loss are circumvented[21,40,41] and continued 4HT-$ROCK^{er}$ [or endogenous ROCK2 activation] adds $ras^{Ha}/ROCK2$-mediated cell-cycle control failures e.g. increased cyclin D,[12,20] too highly proliferative cells with increased susceptibility to mutations, and when overlaid with ROCK2/p-Mypt1-mediated changes to cell motility/tension/ECM, the result is accelerated invasion and metastasis.[7,8]

Another major pathway implicated in $K14.ROCK^{er}/HK1.ras^{1205}$ carcinogenesis involves *NF-κβ*[25] and cross-talk between Rho signalling and canonical *NF-κβ* pathways[9,10] again link to the compensatory p21/p53 responses[11,26] observed in progression. *NF-κβ* signalling mainly associates with inflammatory responses, yet roles also regulate proliferation, apoptosis and cell migration.[25,43] Constitutive NF-κβ overexpression is relatively common, particularly in breast carcinogenesis, making NF-κβ inhibitors another therapeutic avenue.[44] 4HT-treated $K14.ROCK^{er}/HK1.ras^{1205}$ papillomas and $K14.ROCK^{er}$ hyperplasia exhibited elevated basal-layer NF-κβ expression, absent in *HK1.ras* or control histotypes; suggesting early, $ROCK^{er}$-specific roles for *NF-κβ* deregulation. This 4HT-$ROCK^{er}$ –mediated NF-κβ expression is consistent with activation of NF-κβ by Rho-induced, nuclear translocation of p65/RelA; independent of Ras GTPases.[9,10] Whether this is exerting a protective or oncogenic role in this context is unclear,[25] but elevated NF-κβ inflammatory roles would be consistent with

wound promotion, currently associated with fos/Jun/AP1 activation;[45] hence whether fos/AP1 promotes via deregulation of NF-κβ is under investigation.

In addition to inflammatory/wound-promotion roles driving papillomatogenesis, ROCK^{er}-associated NF-κβ expression may influence malignant conversion via circumventing the compensatory p53 responses.[26] In papillomas, NF-κβ and the axis of ROCK2/FAK/β-catenin[5,6] may contribute to the demise of p53, given both NF-κβ[26] and FAK-associated β-catenin[38,46] inhibit p53 expression. These papilloma data thus link NF-κβ with increased DNA mutations/chromosomal instability[25,39] following p53 loss and associated p21 inhibition[47] [below]; and indirectly link ROCK2-mediated NF-κβ to stromal remodelling[25] thus accounting for effects previously observed on expression of ECM molecules such as tenascin C.[48,49] One consequence of p53 loss leading to an altered matrix may involve down-regulated microRNAs,[34] such as miR-200 which regulates cell-cell adhesion molecules[35] and effected ROCK signalling in gastric cancer.[36] Of note, p53-mediated miR-200 expression depended upon AKT levels,[37] consistent with p53 loss driving malignant conversion in tri-genic *HK1.ras/fos/Pten^{flx}* carcinogenesis.[20]

Early NF-κβ expression coupled to p53 down regulation in *K14.ROCK^{er}/HK1.ras^{1205}* papillomas[25,26] would account for increased proliferation, possibly via the NF-κβ responsive element regulating cyclin D[43] and, in sync with ROCK2/ras signalling,[12] add to the increasing pool of cycling cells susceptible to DNA damage/chromosomal re-arrangements. Further following 4HT cessation, as wdSCCs retained NF-κβ expression which continued the inhibition of p53 it helps explain the lack of apoptosis[26,28] and instead, the system attempts to implement a p21-mediated differentiation response[24] leading to the confused/disturbed wdSCC architecture. Previously the combined p53 and p21 responses induced compensatory differentiation levels sufficient to prevent conversion,[23] however, in *K14.ROCK^{er}/HK1.ras^{1205}*

papillomas, NF-κβ/p53 antagonism[25,26] coupled to the axis of ROCK2-associated GSK3β inactivation/increased nuclear β-catenin[5,6,38,46] circumvented the p53 arm.[23] Nonetheless, whilst unable to prevent conversion, persistent p21 remained to inhibited early-stage progression,[20,23,41] until lost, thus releasing ras^{Ha}/ROCK2/NF-κβ synergism to drive progression further.

The cessation experiments clearly demonstrated the ability of p21 to inhibit ROCK2-mediated progression where intense p21 expression confined both ROCK2 and NF-κβ to post-mitotic, supra-basal keratinocytes. This latter result not only shows the requirement for $ROCK^{er}$-mediated NF-κβ expression to facilitate progression, but also demonstrated that p21 responses eliminated NF-κβ expression independent of ROCK2 signalling.[44,47] Furthermore, down-regulation of NF-κβ paralleled increasing basal layer p53 expression[26] which restored the p21/p53-mediated resistance to malignant conversion.[20,23] Indeed, this direct p21-mediated antagonism to NF-κβ signalling was recently demonstrated in liver carcinogenesis where p21 knockout was shown to be pivotal to progression following loss of NEMO, a major NF-kβ pathway regulator.[47] Of relevance to *K14.ROCK^{er}/HK1.ras^{1205}* carcinogenesis, p21 overexpression protected $NEMO^{Dhepa}$ animals against DNA damage,[39,41] whereas p21 knockout accelerated hepato-carcinogenesis in bi-genic $NEMO^{Dhepa}/p21^{null}$ mice,[47] thus implicating NF-κβ in chromosomal damage.[33,39,41,45]

Most major consequences of ROCK2 activation alter the tumour microenvironment and establish a context permissive for stage-specific progression.[1,2,13] Previous *K14.ROCK^{er}* studies demonstrated ROCK-associated collagen deposition resulted in a stiffened ECM and increased tissue rigidity.[5] Similarly human cutaneous SCCs demonstrated ROCK2/p-Mypt1 staining correlated with MLC2 phosphorylation and actomyosin contractility;[6] suggesting a mechano-transduction pathway facilitated progression by providing the mobility/flexibility

necessary to invade tissues with increased rigidity,[6-8] ideas supported by analysis of tenascin C[28-30] and p-Mypt1 inactivation.

Tenascin C is a large ECM/molecule associated with alterations in rigidity that drive progression[27-29] and previously linked with activated Rho/Rock and MAP Kinase signalling.[28,29] Tenascin C expression reflects tumour aggression and metastatic potential[27,48-50] and also associated with deregulated NF-κβ signalling[48] and NF-κβ roles in inflammation.[49] Early 4HT-treated *K14.ROCK^{er}* hyperplasia and *K14.ROCK^{er}/HK1.ras^{1205}* papillomas displayed weak tenascin C levels, despite ROCK^{er}-associated NF-κβ expression, With time and/or p53 loss, increased tenascin C expression appeared in the ECM of both wdSCC and surrounding connective tissue, with intense staining appearing as wdSCCs progressed to SCC.[27-29,48-50] The necessity of continued ROCK^{er} activities for tenascin C expression was shown by cessation experiments and again as endogenous ROCK2/p-Mypt1 appeared, intense tenascin C returned in both tumour and connective tissue ECM to facilitate progression.[28,29] However, following cessation tenascin C repeatedly persisted in connective tissue matrix, but not that of wdSCC tissue; suggesting that once laid down to facilitate conversion, increased tissue rigidity remained. Hence, following cessation ROCK^{er}-dependent wdSCC cells appeared unable to invade, giving rise to the disturbed architecture.

This lack of invasion ability maybe due to loss of ROCK^{er} mediated p-Mypt1 expression[5,6] given that on continued 4HT treatment or rise of endogenous ROCK2, maintenance/return of p-Mypt1 restores p-Mypt1-mediated MLC2 phosphorylation giving increased actomyosin contractility[6] and flexibility/motility for local invasion. Indeed, a feedback mechanism maybe established whereby anomalous ROCK2/p-Mypt1/MLC-mediated changes in local ECM, increase tissue rigidity via altered integrin/FAK/β-catenin signalling and in turn necessitate

ROCK2/p-Mypt1-regulated changes in actinomyosin/MLC expression to provide the motility necessary for transformed cells to invade tissues with increased rigidity.[6,13,28,30]

Collectively these data demonstrate that in the appropriate context of late-stage, highly proliferative $p53^{-ve}/p21^{+ve}/NF\text{-}\kappa\beta^{+ve}$ papillomas, ROCK2 activation co-operates with ras^{Ha} activation to induce malignant conversion. Further ROCK2 and ROCK associated-NFκβ are required to maintain malignant progression to SCC, alongside Mypt1 inactivation/and tenascin c mediated changes in the ECM/motility that facilitate invasion. However, persistent p21 expression is able to counter and inhibit early-stage malignant progression, and if exogenous ROCK activation was lost, significant p21-mediated responses induced a basal-to-suprabasal change in ROCK2/NF-κβ/p-Mypt1 expression and this antagonism also restored p53 tumour suppressor gene functions.

METHODS

Transgenic genotypes and tumour induction.

Transgenic mice expressing a tamoxifen-regulated ROCK2/estrogen fusion protein [*K14.ROCK*^{er}][15] were bred to mice expressing activated ras^{Ha} [*HK1.ras*][17] and maintained as heterozygous transgenes in promotion sensitive *HK1.ras*^{1205} or insensitive *HK1.ras*^{1276} strains.[17] PCR confirmed genotypes, employing primers:
ROCK2 [fwd:5-CGACCACTACCAGCAGAACA-3; rev:5-GACGAACCAACTGCACTTCA-3];
HK1ras [fwd;5-GGATCCGATGACAGAATACAAGC-3;
rev:5-ATCGATCAGGACAGCACACTTGCA-3]. ROCK2 protein activation was achieved by thrice weekly topical treatments of 4-hydroxytamoxifen [330ug 4-HT/20ul ethanol; Sigma] ears and back; control mice received vehicle alone. Each cohort comprised a minimum of 15 male and 5 vehicle controls in repeat experiments; maintained for up to six months. Due to tumour size, 4HT-cessation experiments employed 5 bi-genic animals treated at tagged-ear sites only, at 12 or 14 weeks and maintained for an additional two weeks respectively. All experiments adhered to UK regulations; PPL licenced to DAG.

Histology, Immunofluorescence and Immunohistochemistry

Skin biopsies were fixed in buffered formalin [24hrs @ 4^{o}C] for H&E staining. For immunofluorescence, following antigen retrieval [5 mins. boil/10mM sodium citrate], paraffin sections were incubated [24hrs @ 4^{o}C] with: rabbit anti-K1 [1:100 (Covance)] employing guinea-pig anti-K14 antibodies [1:400 (Fitzgerald)] to delineate epidermis/tumour. Expression was visualized via FITC-labelled anti-rabbit IgG [1:100; (Jackson Labs)] and counterstained with biotinylated goat anti-guinea pig [1:100]/Streptavidin-Texas Red [1:500; (Vector Labs)]. For BrdU labelling, mice were injected IP with 125 mg/kg 5-bromo-4-deoxyuridine [Sigma] 2 hours prior to biopsy. BrdU-labelled cells were identified by incubation [24hrs @ 4^{o}C] with FITC-conjugated anti-BrdU

[1:5(Becton Dickinson)] and counterstained for K14 [above]. For immunohistochemical analysis, following antigen retrieval, paraffin sections were incubated overnight with rabbit anti-p53 [1:50; sc#6243]; $p21^{WAF}$ [1:50; #sc397] at varying dilutions of 1/50, 1/100 and 1/200 in antibody titration experiments; ROCK2 [1:100; sc#5561 (Santa Cruz)], rabbit anti-phospho-$Mypt1^{Thr696}$ [1:50; Millipore]; rabbit anti-tenascin C [1:50; #T2551(Sigma)], and rabbit anti-GFP [1:50; Clonetech] followed by HRP-conjugated goat anti-rabbit [1:100 (Vector)] and visualised by DAB+ [Dako] staining. Photomicrographs employed Axiovision [Zeiss] image capture software.

ACKNOWLEDGEMENTS

We would like to thank Dr. Jean Quinn for help and advice; Stuart Lannigan and Denis Duggan for assistance with animal husbandry. This work was supported by: The Government of Malaysia; the Scott Endowment Fund, Dermatology, Glasgow University; and Cancer Research UK.

The authors state there are no conflicts of interest

Supplementary Information accompanies the paper on the Oncogene website (http://www.nature.com/onc)

References:

1. Olson MF, Sahai E. The actin cytoskeleton in cancer cell motility. *Clin Exp Metastasis* 2009; **26(4):** 273-287.

2. Dufort CC, Paszek MJ, Weaver VM. Balancing forces: architectural control of mechanotransduction. *Nat Rev Mol Cell Biol* 2011; **12:** 308-319.

3. Rath N, Olson MF. Rho-associated kinase in tumorigenesis: re-considering ROCK inhibition for cancer therapy. *EMBO Rep* 2012; **13:** 900-908.

4. Kumper S, Marshall CJ. ROCK-driven actomyosin contractility induces tissue stiffness and tumor growth. *Cancer Cell* 2011; **19:** 695-697.

5. Samuel MS, Lopez JL, McGhee EJ, Croft DR, Strachan D, Timpson P *et al*. Actomyosin-mediated cellular tension drives increased tissue stiffness and β-Catenin activation to induce epidermal hyperplasia and tumor growth. *Cancer Cell* 2011; **19:** 776-791.

6. Ibbetson SJ, Pyne NT, Pollard AN, Olson MF, Samuel MS. Mechanotransduction pathways promoting tumor progression are activated in invasive human squamous cell carcinoma. *The Am J of Path* 2013; **183:** 930-937.

7. Kamai T, Tsujii T, Arai K, Takagi K, Asami H, Ito Y *et al*. Significant association of Rho/ROCK pathway with invasion and metastasis of bladder cancer. *Clin Cancer Res* 2003; **9:** 2632-2641.

8. Sadok A, McCarthy A, Caldwell J, Collins I, Garrett MD, Yeo M *et al.* Rho kinase inhibitors block melanoma cell migration and inhibit metastasis. *Cancer Res* 2015; **75:** 2272-2284.

9. Benitah SA, Valerón PF, Lacal JC. ROCK and nuclear factor-kappaB dependent activation of cyclooxygenase-2 by Rho GTPases: effects on tumor growth and therapeutic consequences. *Mol Biol Cell* 2003; **14:** 3041-3054.

10. Perona R, Montaner S, Saniger L, Sanchez-Perez I, BravoR, Lacal JC. Activation of the nuclear factor-KB by Rho, CDC42, and Rac-1 proteins. *Genes Dev* 1997; **11:** 463-475.

11. Olson MF, Paterson HF, Marshall CJ. Signals from Ras and Rho GTPases interact to regulate expression of p21Waf1/Cip1. *Nature* 1998; **394:** 295-299.

12. Croft DR, Olson MF. The Rho GTPase effector ROCK regulates cyclin A, cyclin D1 and p27Kip1 levels by distinct mechanisms. *Mol Cell Biol* 2006; **26:** 4612-4627.

13. Keely PJ. Mechanisms by which the extracellular matrix and integrin signalling act to regulate the switch between tumor suppression and tumor promotion. *J of Mamm Gland Biol and Neop* 2011; **16:** 205-219.

14. Castellano E, Downward J. RAS interaction with PI3K: more than just another effector pathway. *Genes & Cancer* 2011; **2:** 261-274.

15. Samuel MS, Munro J, Bryson S, Forrow S, Stevenson D, Olson MF. Tissue selective expression of conditionally-regulated ROCK by gene targeting to a defined locus. *Genesis* 2009; **47:** 440-446.

16. Balmain A, Yuspa SH. Milestones in skin carcinogenesis: the biology of multistage carcinogenesis. *J Invest Dermatol* 2014; **134:** 2-7.

17. Greenhalgh DA, Rothnagel JA, Wang XJ, Quintanilla MI, Orengo CC, Gagne TA *et al*. Induction of epidermal hyperplasia, hyperkeratosis, and papillomas in transgenic mice by a targeted v-Ha-ras oncogene. *Mol Carcin* 1993a; **7:** 99-110.

18. Greenhalgh DA, Quintanilla MI, Orengo CC, Barber JL, Eckhardt JN, Rothnagel JA *et al*. Cooperation between v-fos and v-ras^{Ha} induces autonomous papillomas in transgenic epidermis but not malignant conversion. *Cancer Res* 1993c; **53:** 5071-5075.

19. Yao D, Alexander CL, Quinn JA, Porter MJ, Wu H, Greenhalgh DA. PTEN loss promotes ras^{Ha}-mediated papillomatogenesis via dual up-regulation of AKT activity and cell cycle deregulation but malignant conversion proceeds via PTEN-associated pathways. *Cancer Res* 2006; **66:** 1302-1312.

20. Macdonald FH, Yao D, Quinn JA, Greenhalgh DA. PTEN ablation in Ras^{Ha}/Fos skin carcinogenesis invokes p53-dependent p21 to delay conversion while p53-independent p21 limits progression via cyclin D1/E2 inhibition. *Oncogene* 2014; **33:** 4132-4143.

21. Vaezi A, Bauer C, Vasioukhin V, Fuchs E. Actin cable dynamics and Rho/Rock orchestrate a polarized cytoskeletal architecture in the early steps of assembling a stratified epithelium. *Dev Cell* 2002; **3:** 367-381.

22. Lock FE, Hotchin NA. Distinct roles for ROCK1 and ROCK2 in the regulation of keratinocyte differentiation. *PLoS One* 2009; **4:** e8190.

23. Yao D, Alexander CL, Quinn JA, Chan WC, Wu H, Greenhalgh DA. Fos cooperation with PTEN loss elicits keratoacanthoma not carcinoma, owing to p53/p21^{WAF}-induced differentiation triggered by GSK3β inactivation and reduced AKT activity. *J Cell Sc* 2008; **121:** 1758-1769.

24. Topley GI, Okuyama R, Gonzales JG, Conti C, Dotto GP. p21(WAF1/Cip1) functions as a suppressor of malignant skin tumor formation and a determinant of keratinocyte stem-cell potential. *Proc Natl Acad Sci U.S.A.* 1999; **96:** 9089-9094.

25. Karin M, Cao Y, Greten FR, Li ZW. NF-kappaB in cancer: from innocent bystander to major culprit. *Nature Reviews Cancer* 2002; **2:** 301-310.

26. Webster GA., Perkins ND. Transcriptional cross talk between NF-κβ and p53. *Mol. Cell Biol* 1999; **19:** 3485–3495.

27. Lowy CM, Oskarsson T. Tenascin C in metastasis: A view from the invasive front. *Cell Adh Migr* 2015; **9:** 112-124.

28. Sarassa-Renedo A, Tunç-Civelek V, Chiquet M. Role of RhoA/ROCK-dependent actin contractility in the induction of tenascin-C by cyclic tensile strain. *Exp Cell Res* 2006; **312:** 1361-1370.

29. Chiquet M, Sarasa-Renedo A, Tunç-Civelek V. Induction of tenascin-C by cyclic tensile strain versus growth factors: distinct contributions by Rho/ROCK and MAPK signaling pathways. *Biochim Biophys Acra* 2004; **1693:** 193-204.

30. Schlingemann J, Hess J, Wrobel G, Breitenbach U, Gebhardt C, Steinlein P *et al.* Profile of gene expression induced by the tumour promotor TPA in murine epithelial cells. *Int J Cancer* 2003; **104:** 699–708.

31. Milde-Langosch K. The Fos family of transcription factors and their role in tumourigenesis. *Eur J Cancer* 2005; **41:** 2449–2456.

32. Meek DW. Tumour suppression by p53: a role for the DNA damage response? *Nat Rev Cancer* 2009; **9:** 714–723.

33. Zhu J, Sammons MA, Donahue G, Dou Z, Vedadi M, Getlik M. Gain-of-function p53 mutants co-opt chromatin pathways to drive cancer growth. *Nature* 2015; **525:** 206-211.

34. Valastyan S, Weinberg RA. Roles for microRNAs in the regulation of cell adhesion molecules. *J Cell Sci* 2011; **124:** 999-1006.

35. Kim T, Veronese A, Pichiorri F, Lee TJ, Jeon YJ, Volinin S *et al.* p53 regulates epithelial-mesenchymal transition through micro-RNAs targeting ZEB1 and ZEB2. *J Exp Med* 2011; **2008:** 875-883.

36. Zhen B, Liang L, Wang C, Huang S, Cao X, Zha R *et al.* MicroRNA-148a suppresses tumor cell invasion and metastasis by downregulating ROCK1 in gastric cancer. *Clin Cancer Res* 2011; **17:** 7574-7583.

37. Iliopoulos D, Polytarchou C, Hatziapostolou M, Kottakis F, Maroulakoi IG, Struhl K *et al.* MicroRNAs differentially regulated by Akt isoforms control EMT and stem cell renewal in cancer cells. *Sci Signal* 2009; **2:** ra62.

38. Ghosh JC, Altieri DC. Activation of p53-dependent apoptosis by acute ablation of glycogen synthase kinase-3beta in colorectal cancer cells. *Clin Cancer Res* 2005; **11:** 4580-4588.

39. Leonard B, McCann JL, Starrett GJ, Kosyakovsky L, Luengas EM, Molan AM *et al.* The PKC/NF-κB signaling pathway induces APOBEC3B expression in multiple human cancers. *Cancer Res* 2015; **75:** 4538-4547.

40. Warfel NA, El-Deiry WS. p21WAF1 and tumourigenesis: 20 years after. *Curr Opin Oncol* 2013; **25:** 52–58.

41. Barboza JA, Liu G, Ju Z, El-Naggar AK, Lozano G. p21 delays tumour onset by preservation of chromosomal stability. *Proc Natl Acad Sci U S A.* 2006; **103:** 19842–19847.

42. Sahai E, Marshall CJ. Differing models of tumour cell invasion have distinct requirements for Rho/ROCK signalling and extracellular proteolysis. *Nat Cell Biol* 2003; **5:** 711-719.

43. Guttridge DC, Albanese C, Reuther JY, Pestell RG, Baldwin AS Jr. NF-kappaβ controls cell growth and differentiation through transcriptional regulation of cyclin D1. *Mol Cell Biol* 1999; **19:** 5785–5799.

44. Shah KN, Wilson EA, Malla R, Elford HL, Faridi JS. Targeting ribonucleotide reductase M2 and NF-κB activation with Didox to circumvent tamoxifen resistance in breast cancer. *Mol Cancer Ther* 2015; **14:** 2411–2421.

45. Wang J, Ouyang W, Li J, Wei L, Ma Q, Zhang Z *et al*. Loss of tumor suppressor p53 decreases PTEN expression and enhances signalling pathways leading to activation of activator protein 1 and nuclear factor kappaB induced by UV radiation. *Cancer Res* 2005; **65:** 6601-6611.

46. Gao C, Chen G, Kuan SF, Zhang DH, Schlaepfer DD, Hu J. FAK/PYK2 promotes the Wnt/B-catenin pathway and intestinal tumorigenesis by phosphorylating GSK3β. *Elife* 2015; e-pub ahead of print 3 September 2015; doi:10.7554/eLife.10072.

47. Ehedego H, Boekschoten MV, Hu W, Doler C, Haybaeck J, Gabler N *et al*. p21 ablation in liver enhances DNA damage, cholestasis and carcinogenesis. *Cancer Res* 2015; **75:** 1144-1155.

48. Shi M, He X, Wei W, Wang J, Zhang T, Shen X. Tenascin-C induces resistance to apoptosis in pancreatic cancer cell through activation of ERK/NF-κβ pathway. *Apoptosis* 2015; **20:** 843-857.

49. Jachetti E, Caputo S, Mazzoleni S, Brambillasca CS, Parigi SM, Grioni M. Tenascin-C protects cancer stem-like cells from immune surveillance by arresting T-cell activation. *Cancer Res* 2015; **75:** 2095-2108.

50. Oskarsson T, Acharyya S, Zhang XH, Vanharanta S, Tavazoie SF, Morris PG, et al. Breast cancer cells produce tenascin C as a metastatic niche component to colonize the lungs. *Nat Med* 2011; **17:** 867-874.

LEGENDS

Figure 1. Analysis of *K14.ROCK^{er}/HK1.ras^{1205}* carcinogenesis and requirement for tumour promotion stimuli. (**a**) 4HT-treated *K14.ROCK^{er}/HK1.ras^{1205}* mice [14wks], exhibit carcinomas, whereas untreated controls exhibit papilloma clusters. (**b**) At 6wks, 4HT-treated *K14.ROCK^{er}/HK1.ras^{1205}* papilloma formation is identical to (**c**) untreated cohorts. (**d**) Following loss of a wound promotion [ear-tag] stimulus, 4HT-treated *K14.ROCK^{er}/HK1.ras^{1205}* papillomas regress, whilst (**e**) alternate, 4HT-treated *K14.ROCK^{er}/ HK1.ras^{1276}* cohorts exhibit mild ear keratosis only; regardless of wound-promotion and lack papillomas [see supplemental data **Figure S1**]. (**f**) Untreated *K14.ROCK^{er}/HK1.ras^{1205}* tumours exhibit a papilloma histotype, whereas (**g**) 4HT-treated [8/10wks] *K14.ROCK^{er}/HK1.ras^{1205}* tumours possess mixed histotypes of wdSCC [boxed] and papilloma. (**h**) By week 12, 4HT-treated *K14.ROCK^{er}/HK1.ras^{1205}* mice exhibit a uniform wdSCC histotype, with nests of aggressive SCC. (**i)** Higher magnification shows wdSCCs exhibit a ragged/disorganised basal layer indicative of invasion [arrows]; with (**j**) several mitotic figures [arrows] in strands of more aggressive SCC. (**k**) Immunofluorescence analysis of K1[green]/K14[red] expression in 8/9wk 4HT-treated *K14.ROCK^{er}/HK1.ras^{1205}* tumour shows papilloma [below line, left] with green suprabasal expression and red basal layer expression of K14 counterstain; [above line, right] converting papilloma exhibits reduced K1 and a yellow tone. (**l**) 4HT-treated *K14.ROCK^{er}/HK1.ras^{1205}* wdSCCs [12wks] exhibit [right] reduced K1 and [left] increasing red tone on progression to K1^{-ve} SCC (bars: approx. **i-k** ~100µm; **f,g,h**,and **l** ~50µm).

Figure 2. Analysis of ROCK^{er} activation and ROCK 2 isoform expression in pre-neoplastic hyperplasia and temporal, stage-specific progression. *Panel 1:* Epidermal histotype and GFP^{tag}, p-Mypt and ROCK2 isotype expression in 4HT-treated (**a-d**); untreated (**e-h**) *K14.ROCK^{er}* skin or 4HT-treated *HK1.ras* skin (**i-l**). (**a**) 4HT-treated *K14.ROCK^{er}* skin

[20wks] exhibits mild epidermal hyperplasia. (**b**) GFP^{tag} analysis confirms *K14.ROCK^{er}* expression in basal keratinocytes; whilst (**c**) p-Mypt1 expression confirms $ROCK^{er}$ activation. (**d**) Junction between 4HT-treated/untreated skin shows ROCK2-specific antibodies detect endogenous ROCK2 in *spinous* and weak $ROCK^{er}$ expression in basal-layer keratinocytes. (**e**) Untreated *K14.ROCK^{er}* control exhibits normal epidermis; (**f**) positive for GFP-tag but (**g**) little p-Mypt1 expression with (**h**) *spinous*/granular layer ROCK2 expression. (**i**) Control 4HT-treated *HK1.ras^{1205}* skin [4wks] exhibits increased hyperplasia; that (**j**) lacks GFP^{tag} and (**k**) exhibits weak, supra-basal p-Mypt1 or (**l**) supra-basal ROCK2 expression. Diagram indicates epidermal proliferative and differentiating layers and summary of *K14.ROCK^{er}* and *HK1.ras* expression in proliferative, keratin $mK14^{+ve}$ basal layer keratinocytes and supra-basal endogenous ROCK2 expression in differentiated, keratin $mK1^{+ve}$ keratinocytes [bars: ~40µm (**d** and **h**); 60µm (**e-g**; **j-k**); and 100µm (**a-c,l**)]. *Panel 2*: Expression of GFP^{tag} (**a,c,e**) and p-Mypt1(**b,d,** and **f**) in 4HT-treated *K14.ROCK^{er}/HK1.ras^{1205}* papillomas and carcinomas. $ROCK^{er}$ expression was confirmed by detection of GFP^{tag} in (**a**) 4HT-treated wdSCCs [12wks] or (**c**) papillomas [8wks] and absent in (**e**) control 4HT-treated *HK1.ras^{1205}* papillomas. (**b**) Elevated p-Mypt1 expression in wdSCCs [12wks] and (**d**) papillomas confirms $ROCK^{er}$ activation. (**f**) Control 4HT-treated *HK1.ras^{1205}* papillomas exhibit low/supra-basal p-Mypt1 expression [bars: 60µm (**b** and **d**); and 100µm (**a,c,e,** and **f**)]. *Panel 3:* ROCK2 expression in 4HT-treated *K14.ROCK^{er}/HK1.ras^{1205}* carcinogenesis. At low (**a-c**) and higher magnification (**e** and **f**) $ROCK^{er}$/ROCK2 isoforms show strong, elevated expression in all epidermal compartments of (**a**) papillomas [8wks], (**b**) wdSCCs [12wks], (**e**) SCC nests [12wks] and (**c** and **f**) uniform SCCs [16wks]. (**d**) 4HT-treated *HK1.ras^{1205}* papillomas exhibit weak, supra-basal ROCK2 expression. (**g-i**) mK1 expression [green vs K14 (red)], indicative of benign vs malignant state, shows strong, supra-basal expression in

(**g**) benign *HK1.ras* papillomas; (**h**) reduced in wdSCC and (**i**) lost in SCC [bars ~100µm: **a-d**; **g-i**; ~50µm: **e** and **f**].

Figure 3. Analysis of p53, p21 and mitotic index expression in temporal, stage-specific tumour progression. *Panel 1: p53 expression*. (**a**) 4HT-treated *K14.ROCK^{er}/HK1.ras^{1205}* papillomas [8wks] show elevated p53 levels with (**b**) nuclear expression in basal layer keratinocytes. (**c**) Areas of converting 4HT-treated *K14.ROCK^{er}/HK1.ras^{1205}* papillomas [8wks] show p53 expression decreases in strands of basal layer nuclei. (**d**) wdSCCs [10-11wks] exhibit barely detectable, cytoplasmic p53 expression in supra-basal layers. (**e**) SCCs [14wks] are devoid of detectable p53 expression. *Panel 2: p21 expression*. (**a**) 4HT-treated *K14.ROCK^{er}/HK1.ras^{1205}* papillomas [8wks] show elevated p21 expression in all compartments. (**b**) p21 expression persists in wdSCCs [12wks] (**c**) with expression in ROCK^{er}- targeted proliferative basal layers. (**d**) wdSCCs exhibit elevated, uniform p21 in basal and supra-basal layer nuclei. (**e**) SCCs [14wks] loose p21 expression, beginning in nuclei of invasive, disorganised SCC basal cells, resulting in low, supra-basal cytoplasmic expression. *Panel 3*: Immunefluorescence analysis of BrdU labelling and mitotic indices. (**a**) Hyperplastic 4HT-treated *K14.ROCK^{er}* skin [8wks]. (**b**) Normal, untreated *K14.ROCK^{er}* skin [8wks]. (**c**) 4HT-treated *HK1.ras^{1205}* skin [4 wks]. (**d**) 4HT-treated *HK1.ras^{1205}* papillomas [8wks]. (**e)** 4HT-treated *K14.ROCK^{er}/HK1.ras^{1205}* papillomas [8wks] show increased numbers of BrdU positive cells similar to (**f**) 4HT-treated treated *K14.ROCK^{er}/HK1.ras^{1205}* wdSCCs [bars ~150µm: **a**; 100µm: **d,e** and **f**; ~50µm: **c;** ~25µm: **b]**. *Panel 3*: Mitotic indices; quantitation of labelled cells per mm basement membrane. Note: lack of a significant increase in 4HT-treated *K14.ROCK^{er}/HK1.ras^{1205}* carcinomas (71.56 ± 5.25) vs. papillomas (61.50 ± 1.25) [p = 0.561]. Cell proliferation rates were significantly lower in control papillomas [p=<0.05].

Figure 4. Cessation of 4HT treatment. *Panel 1:* Appearance of *K14.ROCK^{er}/HK1.ras^{1205}* tumours at 12wks, 14wks and 2 weeks following 4HT cessation. (**a**) Typical 4HT-treated *K14.ROCK^{er}/HK1.ras^{1205}* mouse at 12wks exhibits a single wdSCC [~225mm^3]. (**b**) At 14wks, treated *K14.ROCK^{er}/HK1.ras^{1205}* cohorts exhibit less keratotic, well vascularised SCCs [~324mm^3]. (**c**) Treated *HK1.ras^{1205}* controls exhibit papilloma clusters [14wks]. (**d**) 4HT cessation for 2 weeks in wdSCCs [12wk] cohorts show similar tumour size [~270mm^3], with increased keratosis and novel tumour outgrowths. (**e**) SCC [14wk cohorts] also show little regression and become larger [~439mm^3]; with novel tumour outgrowths. (**f**) *HK1.ras^{1205}* papilloma clusters remain unchanged [Black lines: plane of dissection; white line: approx.1cm]. *Panel 2:* Analysis of wdSCC [12wk] cohort 2 weeks post 4HT cessation. (**a**) wdSCC [Panel 1**d**] exhibits areas of disturbed tissue architecture [black box] alongside unchanged/SCC area [yellow box]. (**b**) At higher magnification black boxed area exhibits a disordered basal layer, intercellular gaps and increased acanthosis. (**c**) Increased K1 and (**d**) p21 expression appear at sites of disturbed architecture [white/black box]; but not wdSCC/SCC sites [yellow boxes]. (**e**) Elevated p21 expression appears in all layers, including ragged, basal layer nuclei; but [**f**] a serial section lacks detectable p53 expression. (**g** and **h**) ROCK2-specific antibodies show little ROCK^{er} expression in disorganised basal-layers and endogenous ROCK2 is confined to supra-basal keratinocytes. (i) Areas of unchanged wdSCC/SCC exhibit elevated endogenous ROCK2 in all layers. *Panel 3:* Analysis of 14wk SCC cohort 2 weeks post cessation. (**a**) Tumour [panel 1**e**] shows a mix histotype of SCC [(**b-f**) large box] and wdSCC [**(g-j)** small box]. (**b**) SCC areas loose K1 expression and (**c**) p21 levels fade; whilst (**d**) ROCK2-specific antibodies detect elevated endogenous ROCK2 expression giving (**e**) persistent p-Mypt1 expression and (**f**) p21 is lost and (**g**) increased ROCK2 appears in fronts of invasive SCC keratinocytes. (**h**) Former wdSCC histotypes now exhibit elevated K1 with (**i**) elevated p21 in basal-layer nuclei. **(j**) Exogenous

ROCK^{er} fades and endogenous ROCK2 expression becomes supra-basal. (bars: *Panel 2*: **a,c** and **d** ~200µm; **g**~150µm; **f and h ~**100µm**; e** and i~75µm; ; **d** ~50µm. *Panel 3*: **a** ~175µm; **b-e** ~100µm; **h** and **j** ~75µm; **f** and **g** ~50µm; and **i** ~30µm).

Figure 5: Analysis of novel tumour outgrowths. (**a**) Typical tumour outgrowth from Figure 4 panel 1d; line shows dissection plane] exhibits (**b**) typical benign papilloma histotype with (**c**) a standard, strong supra-basal K1 expression and typical basal-layer K14 counterstain. (**d-h**) Anti-p21 titration. (**d**) Employment of routine p21 antibody dilution (1/50) show novel papilloma outgrowths exhibit intense p21 expression in (**e**) both nuclei and cytoplasm of all tumour layers. (**f**) At 1/100 and **(g)** 1/200 dilution, elevated p21 expression is easily detectable again appearing in (**h**) basal layer nuclei and cytoplasm at 1/200 dilutions. (**i-j**) Anti-p53 antibody titration. (**i**) Routine p53 antibody dilution (1/50) demonstrates the return of increasing levels of novel p53 expression also detectable at (**j**) 1/100dil but not (**k**) 1/200 dilution. (**l**) At routine 1/50 dilution, novel p53 re-expression is detected in nuclei and cytoplasm of all tumour layers. (**m**) Low and (**n**) high magnification show novel papillomas express elevated ROCK2 proteins in supra-basal layers only, alongside (**o**) and (**p**) supra-basal p-Mypt expression [bars: **b** and **d** ~150µm; **c,f, i-k, m and o** ~100µm; **c,h,n and p** ~50µm].

Figure 6. Analysis of NF-κβ expression in *K14.ROCK^{er}/HK1.ras^{1205}* carcinogenesis. *Panel 1:* NF-κβ expression in 4HT-treated tumours. (**a**) Treated *K14.ROCK^{er}/HK1.ras^{1205}* papillomas [8wks] display elevated NF-κβ expression. (**b**) Higher magnification [boxed area] shows expression in papilloma basal layer nuclei. (**c**) wdSCC [12wks] exhibit increased NF-κβ staining. (**d**) Higher magnification [boxed area] shows intense NF-κβ expression in both nuclei and cytoplasm of invasive cells. (**e**) Strong NF-κβ [14wks] is maintained in [p21^{ve}/K1^{-}

^{ve}] aggressive, invasive SCC cells and (**f**) becomes less cytoplasmic with (**g**) strong nuclear expression. (**h**) Untreated *K14.ROCK^{er}/HK1.ras^{1205}* papillomas [12wks] exhibit weak staining, with few cells expressing nuclear NF-κβ. (**i**) 4HT-treated *K14.ROCK^{er}* hyperplasia express detectable NF-κβ sporadic nuclear expression in basal-layer keratinocytes. (**j**) *HK1.ras^{1205}* hyperplasia expresses little NF-κβ. *Panel 2:* NF-κβ expression following cessation of 4HT. (**a**) wdSCCs (serial section; Figure 4: panel **2a,c** and **d**], shows elevated NF-κβ expression in all layers, with (**b**) persistent nuclear expression in areas of [p21^{+ve}/K1^{+ve}] disturbed architecture. (**c**) Invasive SCCs [14wk/2wk without 4HT; Figure 4: panel 3**]** exhibit elevated NF-κβ expression, paralleled by (**d**) elevated endogenous ROCK2 expression. (**e**) At low and (**f**) higher magnification, papilloma outgrowths [serial sections from Figure 5] show reduced basal layer NF-κβ expression with few NF-κβ^{+ve} nuclei, now confined to a supra-basal expression profile. (**g**) Endogenous ROCK2 parallels this p21-restricted, supra-basal expression profile [bars: Panel 1 **a** and **c** ~200µm; **b,d,e,h** and **j** ~100µm; **f,g** and **I** ~50µm; Panel 2: **a,c-e** and **g** ~100µm; **b** and **f** ~50µm].

Figure 7. Analysis of tenascin C and p-Mypt1 expression in *K14.ROCK^{er}/HK1.ras^{1205}* carcinogenesis. *Panel 1:* Tenascin C expression in 4HT-treated tumours. (**a**) Treated and (**b**) untreated *K14.ROCK^{er}/HK1.ras^{1205}* papillomas [8wks] display low tenascin C levels except in sporadic dermal cells. (**c**) At 12wks wdSCC express elevated tenascin C in connective tissue, with patches of intense staining in carcinoma. (**d** and **e**) At higher magnification, intense tenascin C staining is prominent in supra-basal ECM, with elevated staining in the surrounding tissues. (**f**) 4HT-treated *HK1.ras^{1205}* papillomas [12wks] exhibit low tenascin C expression. (**g**) 4HT-treated *K14.ROCK^{er}* hyperplasia exhibits tenascin C staining in dermal ECM unlike (**h**) early *HK1.ras^{1205}* hyperplasia. (**i**) Following 4HT cessation, wdSCC/SCCs [14wks; Figure 4 panel 3] show (**j**) intense tenascin C staining in SCC ECM. (**k**) wdSCC histotypes loose tenascin C expression in tumour tissues but expression is retained in connective tissue ECM.

(**l**) Novel papilloma outgrowths [Figure 5] display patches of tenascin C and weak dermal ECM staining. *Panel 2:* p-Mypt1 expression in 4HT-treated tumours. (**a**) Treated *K14.ROCK^{er}/HK1.ras^{1205}* papillomas [8wks] display elevated p-Mypt1 compared to (**b**) weak expression in untreated controls. (**c**) 4HT-treated wdSCCs exhibit increased p-Mypt1 inactivation. Following 4HT cessation (**d**) ROCK2-positive SSC histotypes retain elevated p-Mypt1 expression [boxed area; panel 1J] (**e**) ROCK2^{er} negative/ROCK2-suprabasal wdSCC histotype [boxed area, panel **1k**] exhibits reduced supra-basal p-Mypt1. (**f**) Papilloma outgrowths display p-Mypt1 expression confined to [ROCK2/NF-κβ-positive] supra-basal layers [bar: Panel 1: **c** and **i** ~250µm; **a,b** and **j-l** ~150µm; **d** and **f** ~100µm; **e,g** and **h** 50µm. Panel 2: all ~100µm].

Figure 1

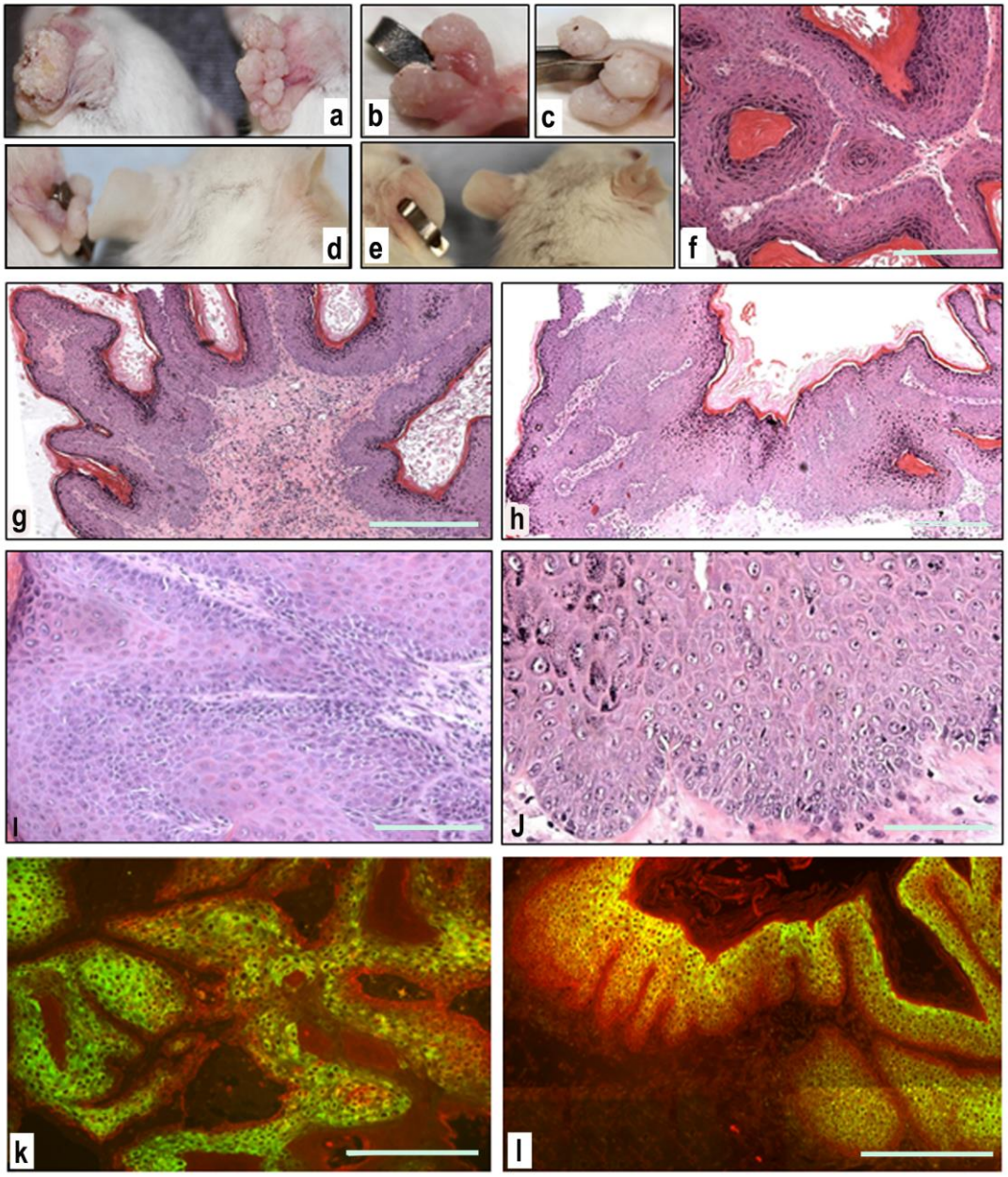

Figure2

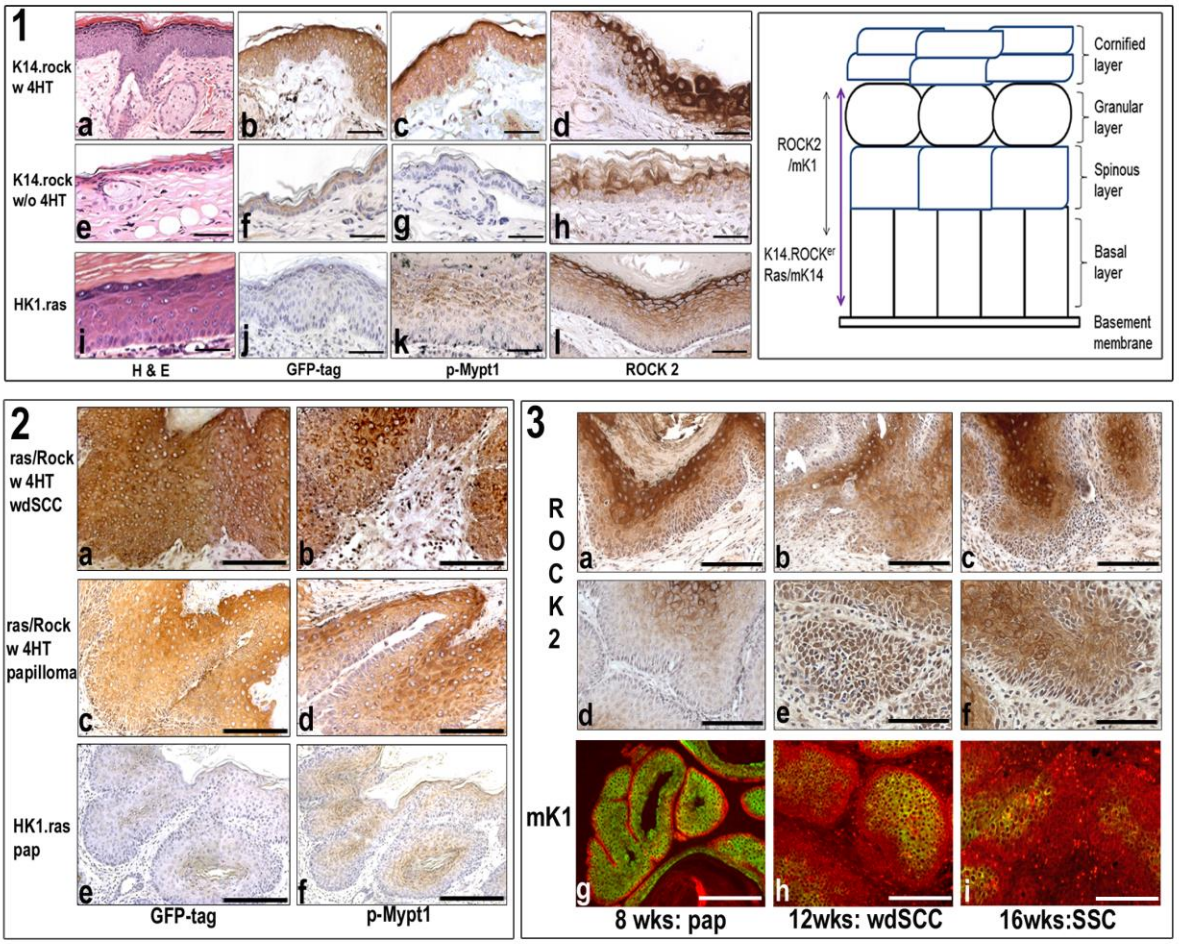
1
K14.rock w 4HT
K14.rock w/o 4HT
HK1.ras
a
b
c
d
e
f
g
h
i
j
k
l
H & E
GFP-tag
p-Mypt1
ROCK 2
Cornified layer
Granular layer
Spinous layer
Basal layer
Basement membrane
ROCK2 /mK1
K14.ROCK^{er} Ras/mK14
2
ras/Rock w 4HT wdSCC
ras/Rock w 4HT papilloma
HK1.ras pap
GFP-tag
p-Mypt1
3
ROCK2
mK1
8 wks: pap
12wks: wdSCC
16wks:SSC

Figure 3

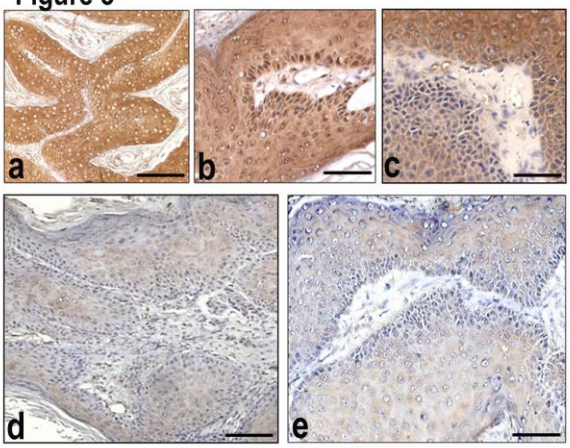

Panel 1: p53 expression

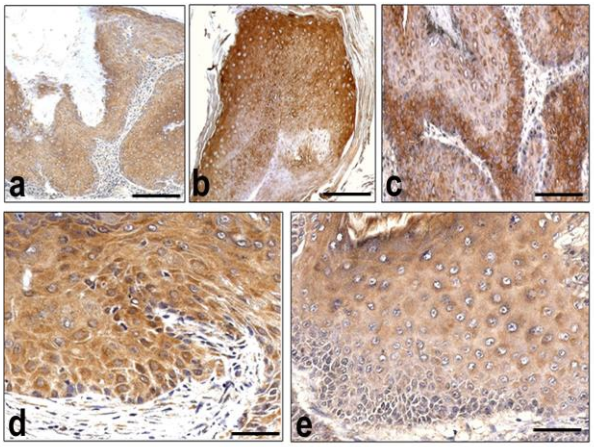

Panel 2: p21 expression

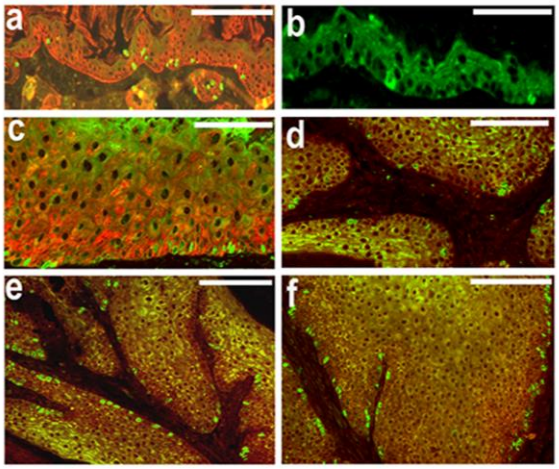

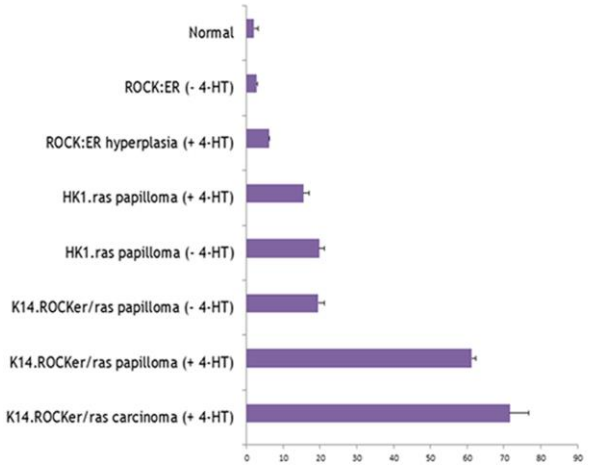

Panel 3: BrdU labelling and mitotic index

figure 4

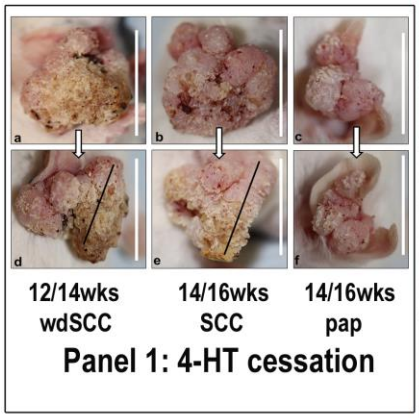

Panel 1: 4-HT cessation

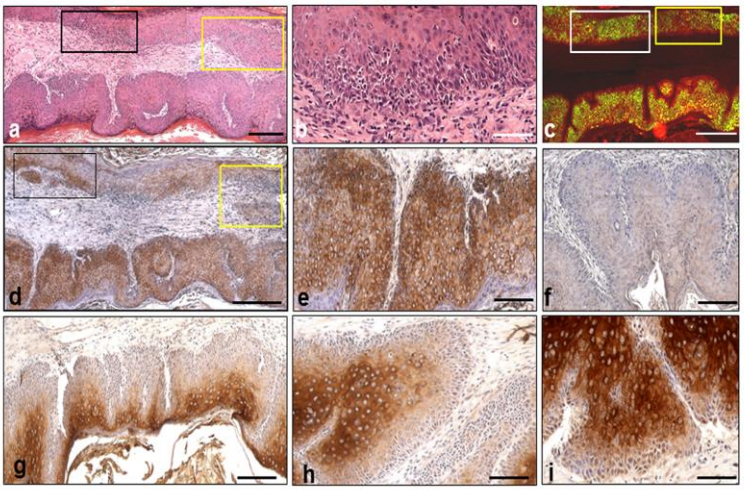

Panel 2: 4-HT cesation @ 12/14wks

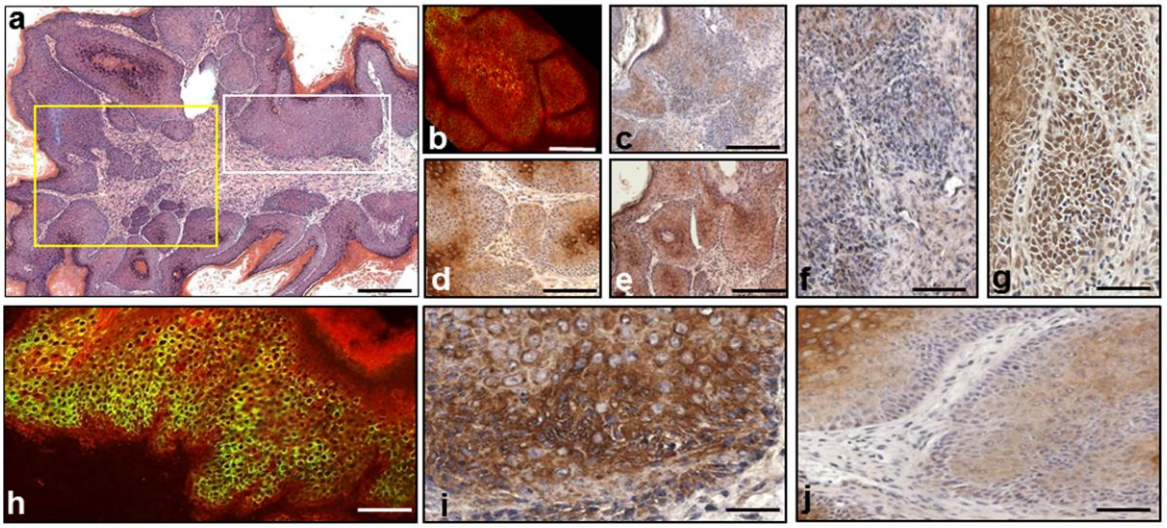

Panel 3: 4-HT cessation @14/16wks

Figure 5

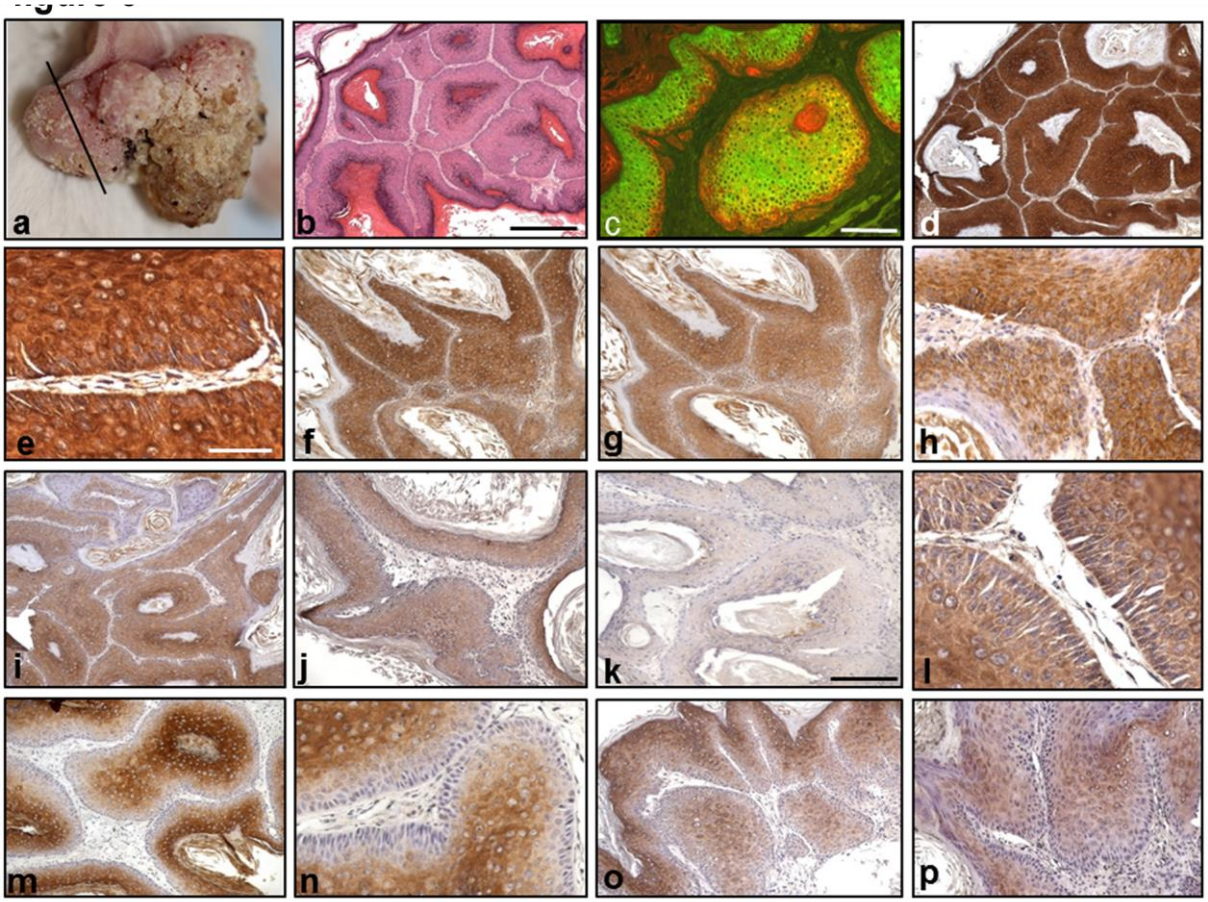

Figure 6

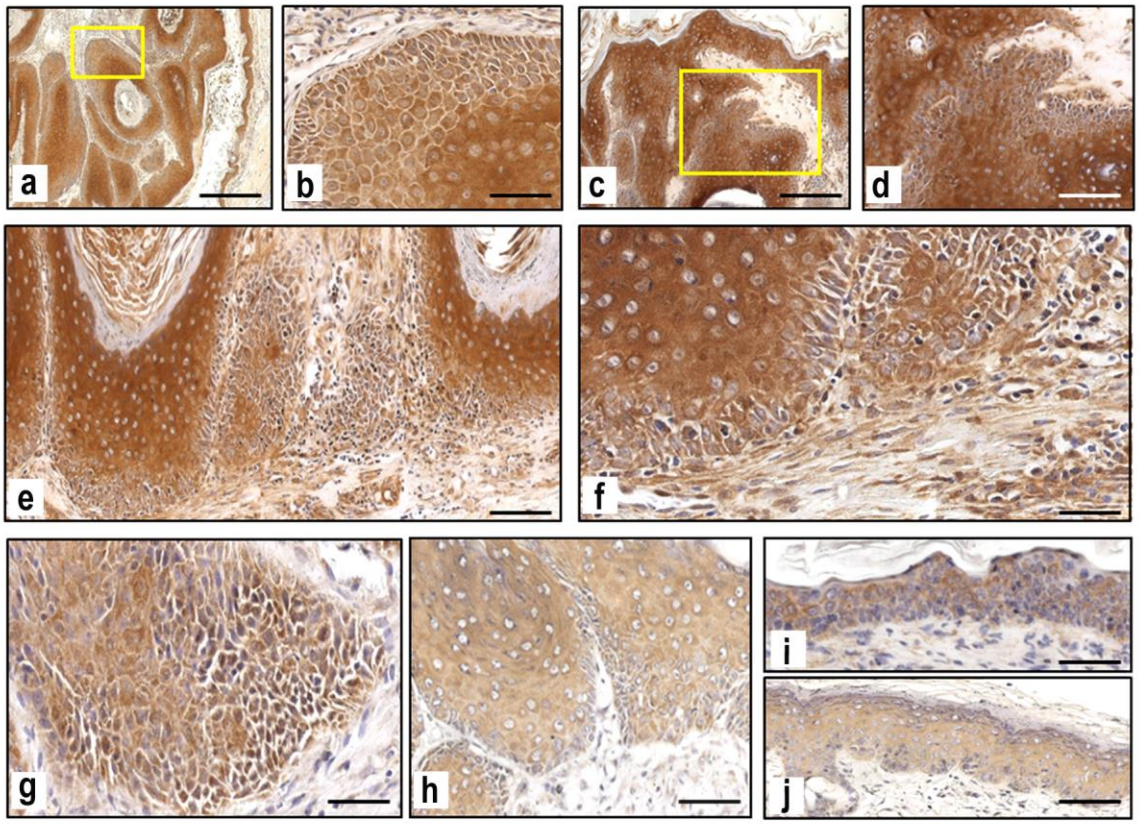

Panel 1: NF-κβ expresssion at 8,12 &14wks 4-HT

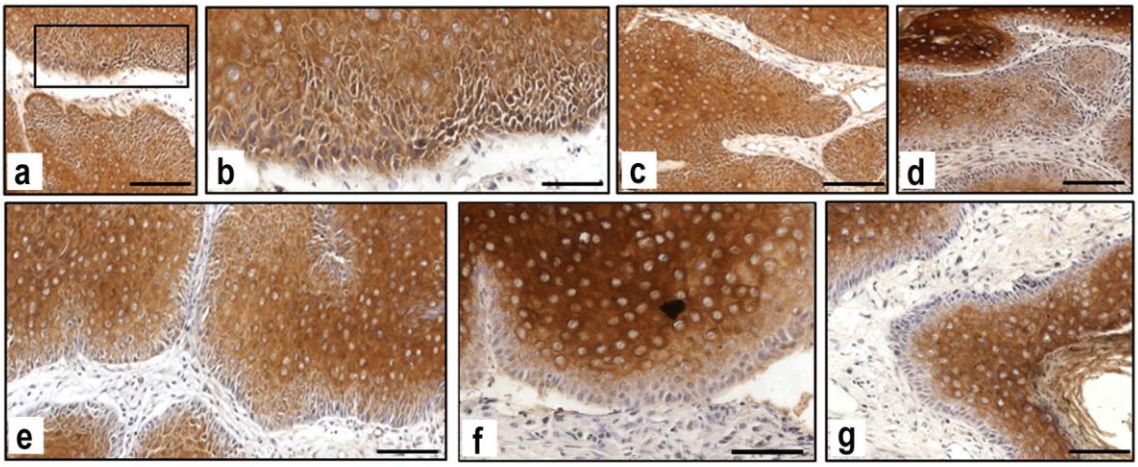

Panel 2: NF-κβ expresssion ceased 4-HT treatment

Figure 7

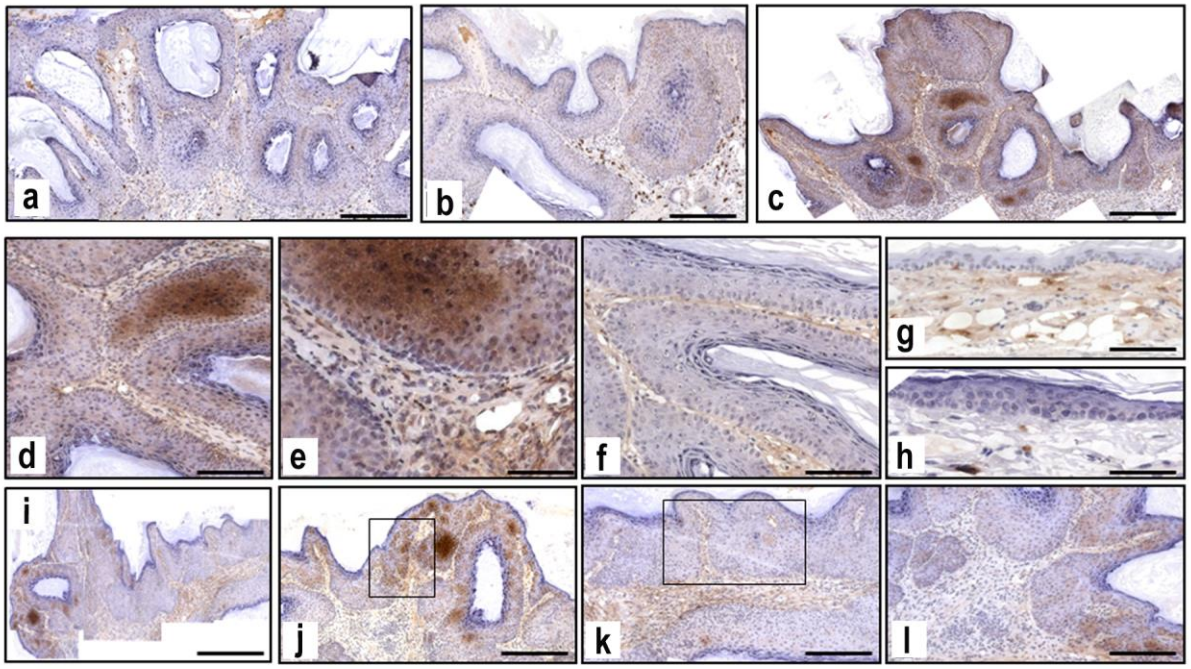

Panel 1: Tenascin C

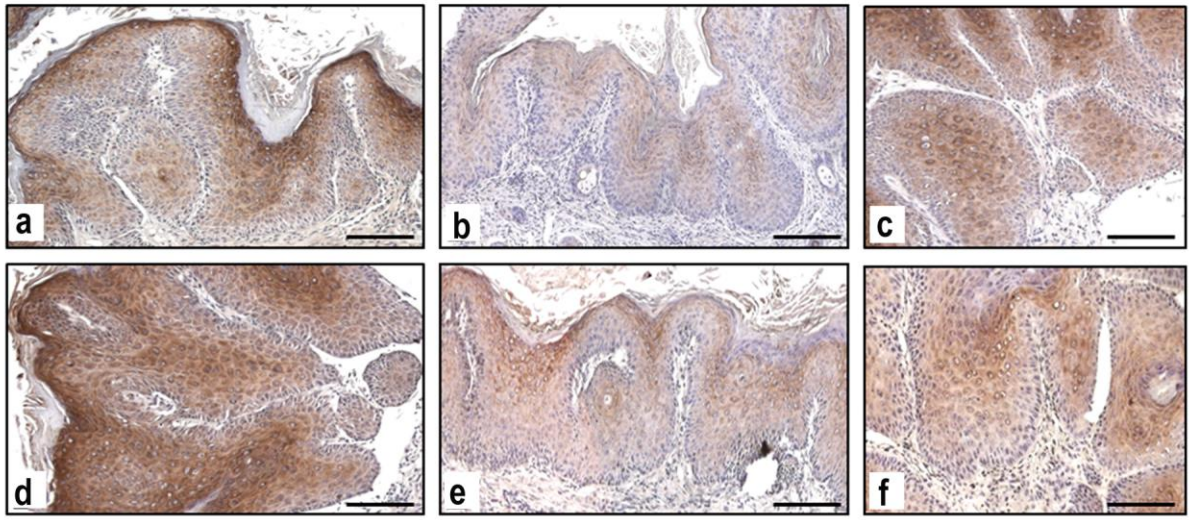

Panel 2: p-Mypt 1